AD-A066 602 STATE UNIV OF NEW YORK AT BUFFALO DEPT OF CHEMISTRY F/G 9/1
NON-WETTING MATERIALS FOR FABRICATION OF FUEL CELL ELECTRODES.(U)
DEC 77 R MACK, S BRUCKENSTEIN DAAG53-76-C-0026

UNCLASSIFIED NL

| OF |
AD
A066602

END
DATE
FILMED
5-79
DDC

END
DATE
FILMED
5-79
DDC

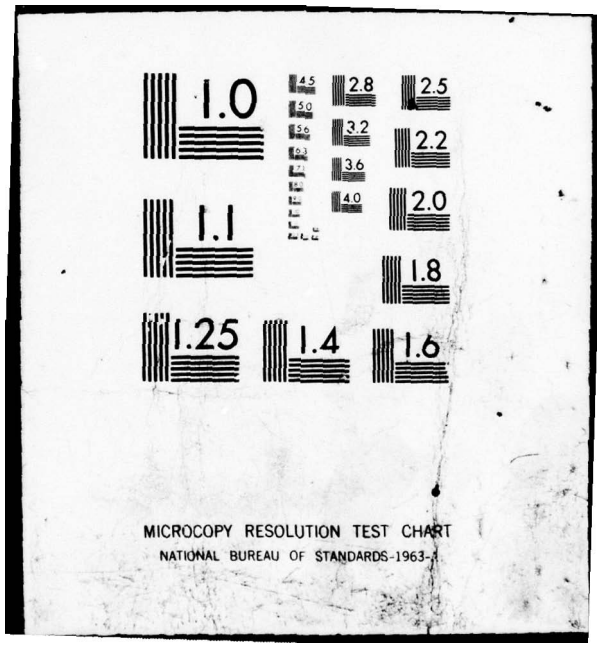
1.0
1.1
1.25
1.4
1.6
1.8
2.0
2.2
2.5
2.8
3.2
3.6
4.0
4.5
5.0
5.6
MICROCOPY RESOLUTION TEST CHART
NATIONAL BUREAU OF STANDARDS-1963-A

UNCLASSIFIED

NON-WETTING MATERIALS FOR FABRICATION OF FUEL CELL ELECTRODES.

FINAL REPORT

By

Robert Mack
and
Stanley Bruckenstein

December 1977

Prepared for

U.S. Army Mobility Equipment
Research and Development Center
Ft. Belvoir, Virginia 22060

Contract No. DAAG53-76-C0026

Prepared by

Chemistry Department
State University of New York at Buffalo
Buffalo, New York 14214

UNCLASSIFIED

NOTICES

DISTRIBUTION STATEMENT

THIS DOCUMENT HAS BEEN APPROVED FOR PUBLIC RELEASE AND SALE.
ITS DISTRIBUTION IS UNLIMITED.

DISCLAIMERS

THE FINDINGS IN THIS REPORT ARE NOT TO BE CONSTRUED AS AN OFFICIAL DEPARTMENT OF THE ARMY POSITION, UNLESS SO DESIGNATED BY OTHER AUTHORIZED DOCUMENTS.

THE CITATION OF TRADE NAMES OF MANUFACTURERS IN THIS REPORT IS NOT TO BE CONSTRUED AS OFFICIAL GOVERNMENT ENDORSEMENT OR APPROVAL OF COMMERICAL PRODUCTS OR SERVICES REFERENCED THEREIN.

DISPOSITION

DESTROY THIS REPORT WHEN IT IS NO LONGER NEEDED.
DO NOT RETURN IT TO THE ORIGINATOR.

SECURITY CLASSIFICATION OF THIS PAGE (When Data Entered)

REPORT DOCUMENTATION PAGE

READ INSTRUCTIONS BEFORE COMPLETING FORM

1. REPORT NUMBER

2. GOVT ACCESSION NO.

3. RECIPIENT'S CATALOG NUMBER

4. TITLE (and Subtitle)

(6) Non-Wetting Materials for Fabrication of Fuel Cell Electrodes.

5. TYPE OF REPORT & PERIOD COVERED

(9) Final Technical Report, December 30, 1977

6. PERFORMING ORG. REPORT NUMBER

7. AUTHOR(s)

Mack, Robert and Bruckenstein, S.

(10) Robert/Mack Stanley/Bruckenstein

8. CONTRACT OR GRANT NUMBER(s)

DAAG53-76-C0026

(15) DAAG53-76-C-0026

9. PERFORMING ORGANIZATION NAME AND ADDRESS

Chemistry Department
SUNY at Buffalo
Buffalo, New York 14214

10. PROGRAM ELEMENT, PROJECT, TASK AREA & WORK UNIT NUMBERS

11. CONTROLLING OFFICE NAME AND ADDRESS

U.S. Army Mobility Equipment Research and Development Command, Fort Belvoir, Virginia

(11) 12. REPORT DATE

December 1977

13. NUMBER OF PAGES

51 + v

14. MONITORING AGENCY NAME & ADDRESS (if different from Controlling Office)

(12) 64p.

15. SECURITY CLASS. (of this report)

Unclassified

15a. DECLASSIFICATION/DOWNGRADING SCHEDULE

16. DISTRIBUTION STATEMENT (of this Report)

Approved for public release; distribution unlimited

17. DISTRIBUTION STATEMENT (of the abstract entered in Block 20, if different from Report)

18. SUPPLEMENTARY NOTES

19. KEY WORDS (Continue on reverse side if necessary and identify by block number)

Electrochemistry, Fuel Cell, Electrodes, Electrolytes, ion exchange membrane, trifluoromethene sulfonic acid monohydrate, phosphoric acid.

20. ABSTRACT (Continue on reverse side if necessary and identify by block number)

A study of propane electrooxidation on a platinum coated ion exchange membrane was conducted in both 85% phosphoric acid and trifluoromethane-sulfonic acid monohydrate (TFMSA). The phosphoric acid system's propane electrooxidation current were characterized with respect to temperature,

DD FORM 1 JAN 73 1473 EDITION OF 1 NOV 65 IS OBSOLETE

Unclassified

SECURITY CLASSIFICATION OF THIS PAGE (When Data Entered)

400 352

20. Abstract (Continued)

propane flow rate and oxidation potential. Then, the propane electrooxidation currents of the TFMSA system were determined and compared to the phosphoric acid system. The steady state currents in the TFMSA solvent were two times greater than in the 85% H_3PO_4 acid solvent.

Steady state hydrogen electrooxidation current measurements were made in both solvents and compared to the propane electrooxidation currents to estimate the practicability of propane electrooxidation. On a mole basis, the propane currents were 1/143 of the hydrogen currents.

Two problems inherent in the TFMSA system were uncovered during these experiments.

The conductance of the TFMSA solvent was about one tenth of the conductance of the phosphoric acid solvent. Conductance measurements of the solvated ion exchange membranes were also evaluated.

Platinum, the electrocatalyst for propane electrooxidation was found to dissolve (be oxidized) under conditions that may occur in a propane fuel cell. Linear voltage scan experiments using a coiled platinum wire electrode were conducted and verified the platinum dissolution observed in the PtIEM experiments.

NON-WETTING MATERIALS FOR FABRICATION OF FUEL CELL ELECTRODES.

FINAL REPORT

By

Robert Mack
and
Stanley Bruckenstein

December 1977

Prepared for

U.S. Army Mobility Equipment
Research and Development Center
Ft. Belvoir, Virginia 22060

Contract No. DAAG53-76-C0026

Prepared by

Chemistry Department
State University of New York at Buffalo
Buffalo, New York 14214

TABLE OF CONTENTS

Table of Contents Continued

CHAPTER III

CHAPTER IV

CHAPTER V

CHAPTER VI

FOREWARD

This work is sponsored by the U.S. Army Mobility Equipment Research and Development Center, Fort Belvoir, Virginia, under Contract No. G53-76-60026 in order to develop a technology which will facilitate the development of an efficient military fuel cell operating on ambient air and hydrocarbon fuels using trifluoromethanisulfonic acid as solvent.

LIST OF FIGURES

LIST OF TABLES

ABSTRACT

A study of propane electrooxidation on a platinum coated ion exchange membrane was conducted in both 85% phosphoric acid and trifluoromethanesulfonic acid monohydrate (TFMSA). The phosphoric acid system's propane electrooxidation currents were characterized with respect to temperature, propane flow rate and oxidation potential. Then, the propane electrooxidation currents of the TFMSA system were determined and compared to the phosphoric acid system. The steady state currents in the TFMSA solvent were two times greater than in the 85% H_3PO_4 acid solvent.

Steady state hydrogen electrooxidation current measurements were made in both solvents and compared to the propane electrooxidation currents to estimate the practicability of propane electrooxidation. On a mole basis, the propane currents were 1/143 of the hydrogen currents.

Two problems inherent in the TFMSA system were uncovered during these experiments.

The conductance of the TFMSA solvent was about one tenth the conductance of the phosphoric acid solvent. Conductance measurements of the solvated ion exchange membranes were also evaluated.

Platinum, the electrocatalyst for propane electrooxidation was found to dissolve (be oxidized) under conditions that may occur in a propane fuel cell. Linear voltage scan experiments using a coiled platinum wire electrode were conducted and verified the platinum dissolution observed in the PtIEM experiments.

CHAPTER I

INTRODUCTION

A. Historical

In recent years, much research has been devoted toward the development of an efficient propane fuel cell. A major breakthrough was made by Grubb and Niedrach in 1963 when they found efficient electro-oxidation of propane occurs on platinum electrodes at 150°C in 14.6 M H_3PO_4 (1). Adams and Barger later reported that a 1000% increase in propane oxidation current densities could be obtained in trifluoro-methane sulfonic acid monohydrate (TFMSA) as compared to 14.6 M H_3PO_4(2). These currents were recorded five minutes after establishing the constant potential in the range from 0.3 V to 0.7 V vs. the DHE. The highest current densities obtained in TFMSA for these experiments were 32.0 $\mu A/cm^2$ at 135°C on a platinum mesh electrode.

Another major development in fuel cell technology was made by Grubb in 1957 when he suggested that an ion exchange membrane (IEM) could be used as the electrolyte in fuel cells (3). Since then, IEM's have found extensive use in hydrogen-oxygen fuel cells and water electrolysis systems.

B. Purpose

The purpose of this research was to study a platinum coated ion exchange membrane (PtIEM) in TFMSA to determine if this system would function more efficiently as a propane fuel cell than a conventional porous platinum-Teflon structure in H_3PO_4. The latter structure cannot be used in TFMSA because this solvent floods the pores of the platinum-Teflon structure.

Steady state propane electrooxidation current densities were

determined at the PtIEM electrode in both TFMSA and 85% H_3PO_4 solvents at various temperatures, propane flow rates, and potentials. These current densities were compared with hydrogen electrooxidation current densities in 85% H_3PO_4 and TFMSA. The current density comparisons were used to evaluate the PtIEM electrode's prospects for use as a fuel cell electrode in TMFSA.

CHAPTER II

EXPERIMENTAL

A. Apparatus and Equipment

1. Electrolysis Cell

The electrolysis cell used in this investigation is shown in Figure 1. It was a relatively air-tight system of 20 ml. volume with a gas bubbler fixed in position near the PtIEM electrode. The auxillary compartment was isolated from the main cell by a 12 mm diameter medium glass frit. A coiled platinum wire was used as the auxilliary electrode.

The polarized hydrogen electrode (PHE), described by Giner (4) was used as the reference electrode in all experiments reported here. The current between the two PHE's platinum coiled wire electrodes was maintained at 2.5 mA by the control circuit shown in Figure 1.

2. Linear Scan Working Electrode.

The coiled 24 gauge platinum wire electrode, shown inside the 14/35 standard taper joint in the electrolysis cell of Figure 1, was used as the working electrode in all linear potential scan experiments. The coiled platinum wire was sealed in the 14/35 standard taper joint so that it could be placed in a position similar to the PtIEM electrode also used with this cell.

3. Conductance Cell

A sketch of the cell used for conductance measurements is shown in Figure 2. The two coiled platinum wire electrodes were sealed rigidly in glass so as to be fixed relative to each other.

The 14/35 standard tapered joint secured a PtIEM disk be-

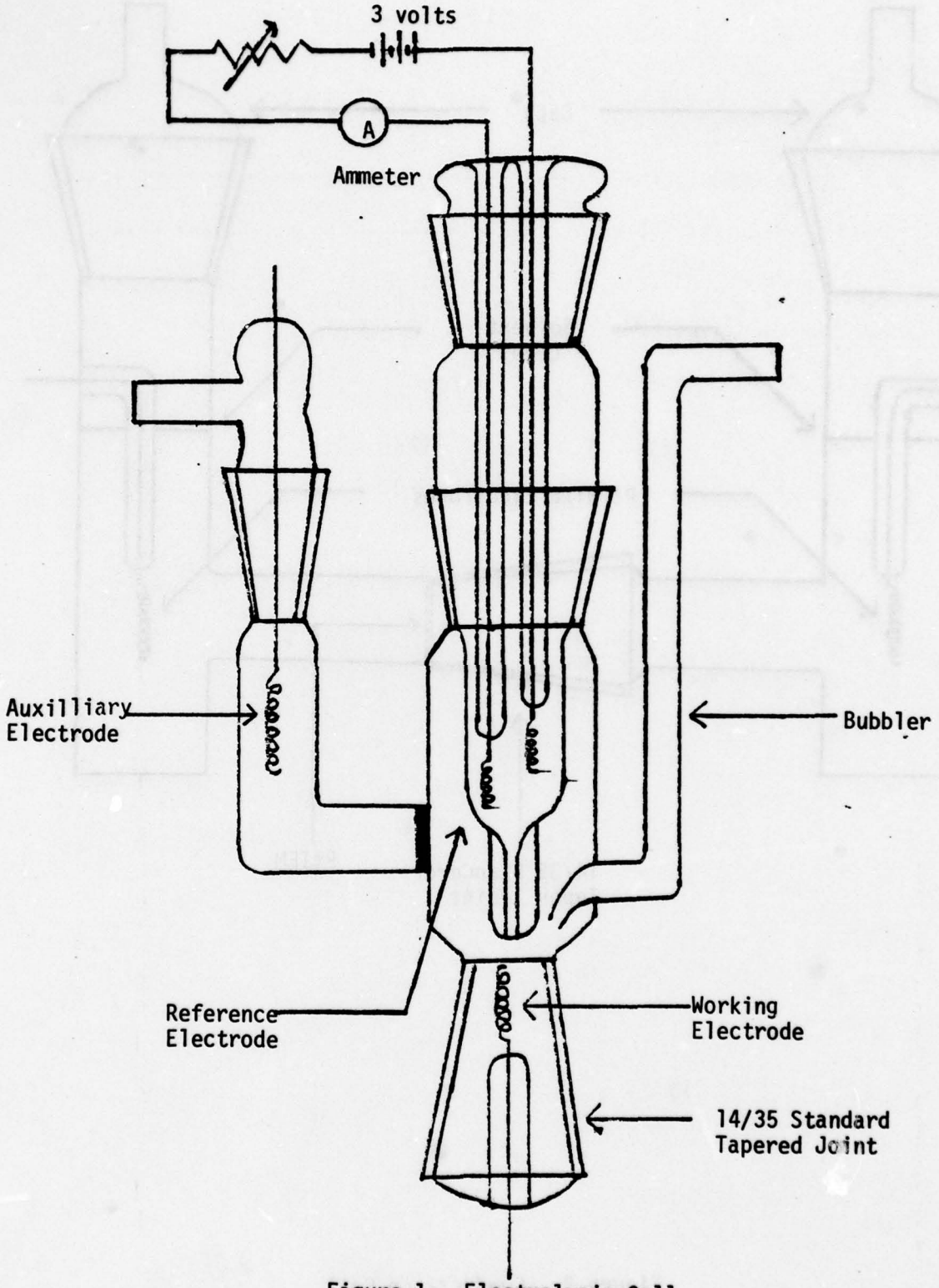

Figure 1. Electrolysis Cell

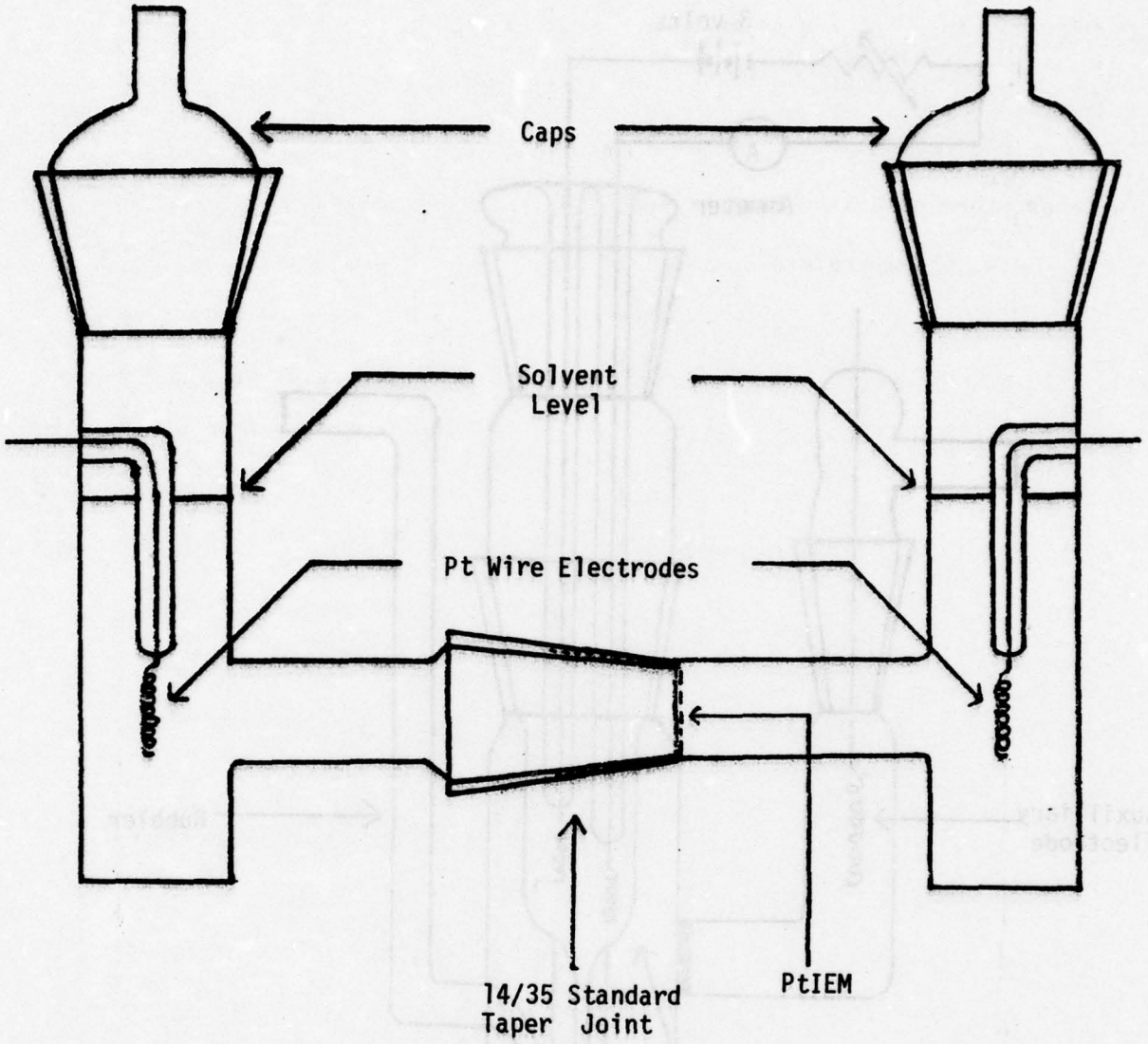

Figure 2. Conductance Cell

tween the two half cells filled with solvent. A piece of PtIEM larger in diameter than the end of the inner part of the 14/35 joint was placed on the end of the inner joint, and the inner joint inserted into the outer joint. The edges of the PtIEM were compressed between the joint surfaces, forming a liquid-tight seal.

4. Temperature Control

Temperatures were controlled to within $\pm$ 1°C for all experiments by placing the electrolysis and conductance cells in a Model SW-11TA Blue M oven. Temperatures used ranged from 120°C to 140°C in these experiments.

5. Gas Flow System

Gas flow and proportioning were controlled by a stainless steel Union Carbide Linde proportionator, model FM-4631, and stainless steel Union Carbide Linde flow meter, model FM-4311. In some experiments, a 500 ml. gas saturator containing distilled water was connected after the flow meter. Connections in the gas inlet system external to the oven were made with 1/4 inch inner diameter tygon tubing.

The part of the gas inlet system contained in the oven was made of 6 mm diameter glass tubing. When gases were preheated, a 15 foot coil of 1/4 inch outside diameter copper tubing was incorporated into the gas inlet system and was placed in the oven immediately next to the cell.

Teflon shrink tubing was used to make all required interconnections in the gas flow system and the gas inlet and outlet ports of the electrodes (Figures 6 and 7).

The gases studied passed over the PtIEM electrode's surface and then through the gas exit port to a 6 mm glass tube which exited the oven into a fume hood.

6. Electronic Support Systems

A conventional three electrode potentiostat was used for all experiments requiring potential control. This potentiostat circuit is described elsewhere (5). The linear potential scan programs required for this potentiostat were provided by an analog ramp generator having independent ramping-rate and potential-limit controls.

An Industrial Instrument Model RC-216B2 conductivity bridge was used for most of the conductance measurements. This bridge circuit was operated at 1000 Hz. Other measurements involving cell resistance were made using the circuit shown in Figure 3A. It determined cell resistance ratios, for the purpose described later. Figure 3B is the equivalent circuit of Figure 3A, provided cell capacitance is negligible. A constant amplitude 1 KHz sine wave was applied to the cell using a Heathkit Model IG18 sine-square wave audio signal generator. The peak to peak sine wave ampltiudes across the cell and at the reference electrode were measured with a Tektronix Type 502 Dual-Beam oscilliscope.

For platinum dissolution studies, the bipolar constant current generator shown in Figure 4 was utilized. This generator outputs a symmetric square wave at a frequence of 0.1 Hz with an adjustable peak to peak current centered at zero.

A data logger was used to digitally record currents for long term steady state studies. These currents were measured by a Fluke 8000A Digital Multimeter with its output fed to a Fluke 2010 A Printer. The paper tape printer recorded this current and the time whenever a gating pulse was sent to it from a precision digital clock. The clock could generate pulses at time intervals from ten pulses per second to

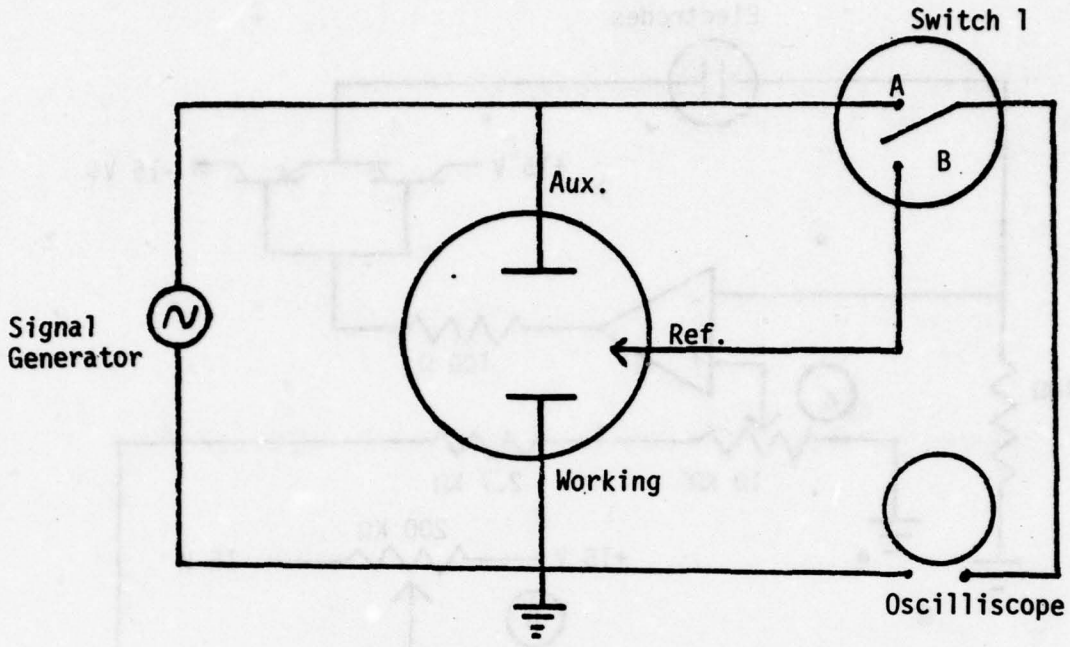

Figure 3A. Physical Circuit

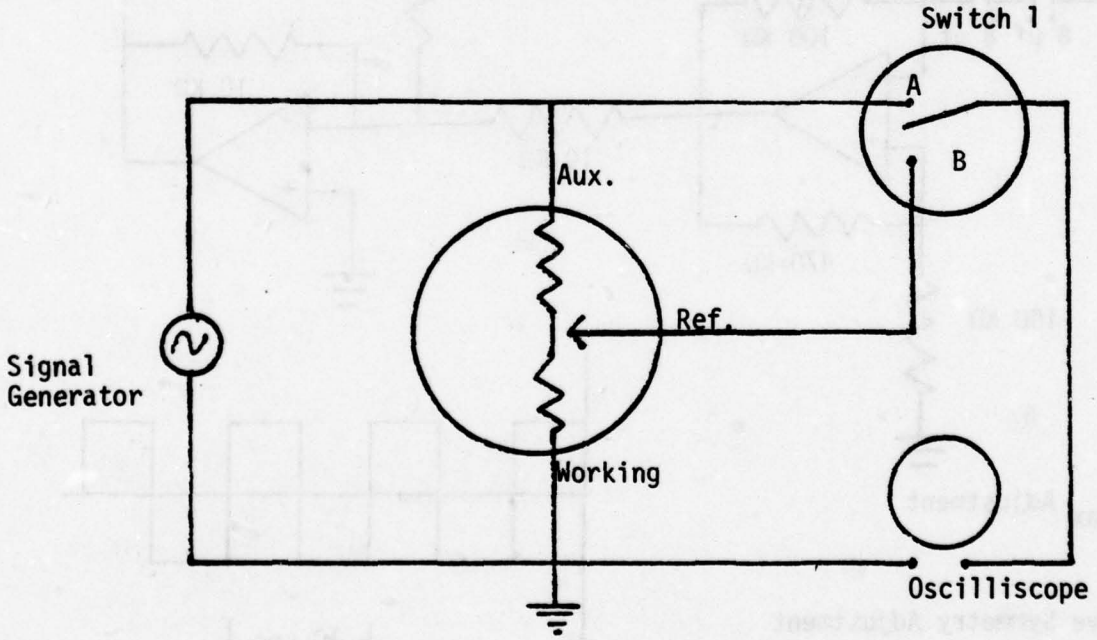

Figure 3B. Equivalent Circuit

Figure 3. Resistance Ratio Determination

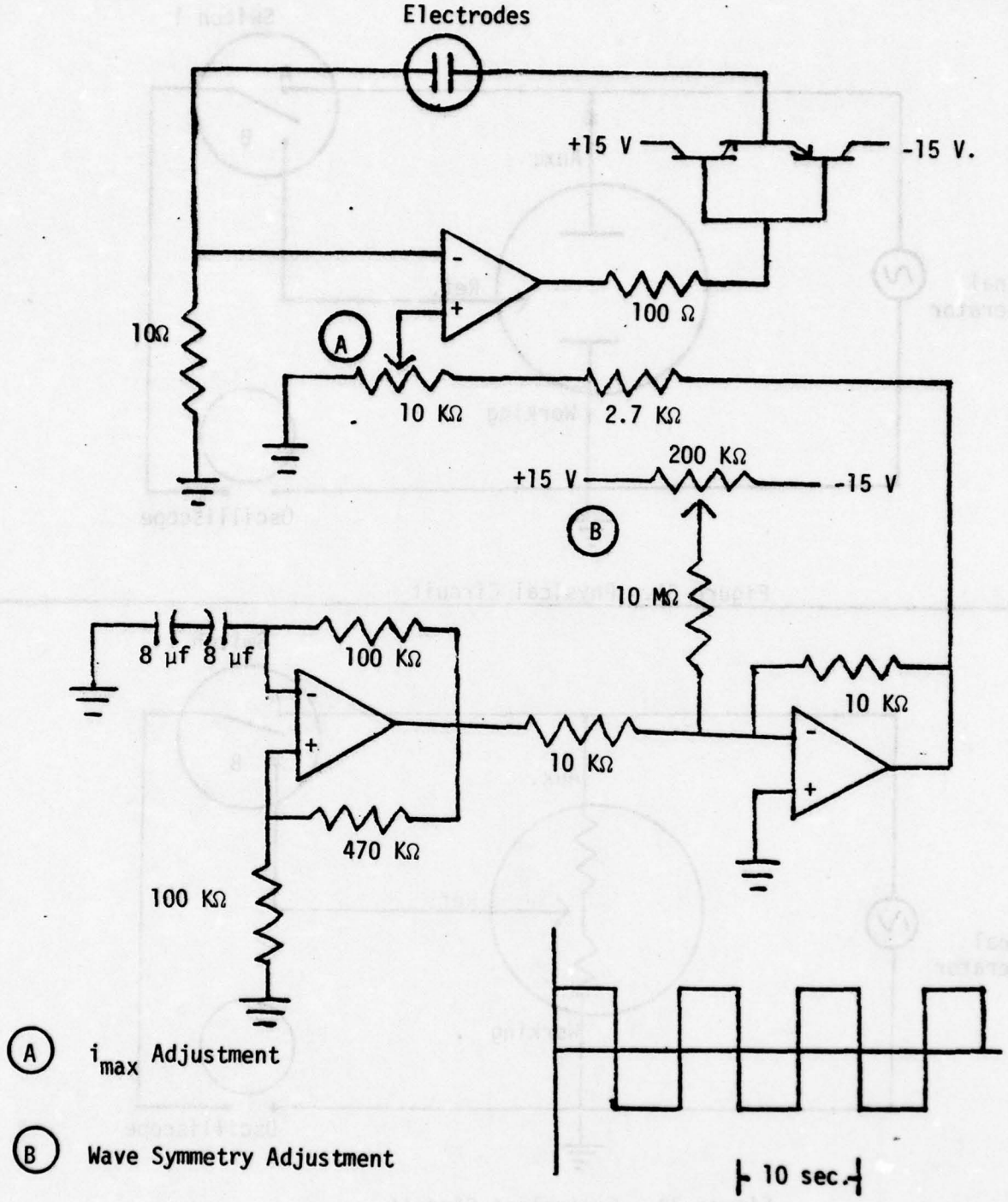

Figure 4. Bipolar Constant Current Circuit Diagram

one pulse per hour.

"Steady-State" currents and potentials were measured with a Keithley Model 180 digital multimeter.

Current-potential curves were recorded on a EAI model 1130 X-Y Variplotter.

B. Chemicals

1. Solvents

Fisher Scientific Company 85% H_3PO_4 was used without further purification.

TFMSA was prepared from 3M Brand Trifluoromethanesulfonic acid FC-24. Equimolar quantities of trifluoromethanesulfonic acid and Millipore Milli-Q™ water were mixed in a round bottom flask and connected to a simple distillation apparatus. The mixture was distilled collecting only the fraction between 200°C and 220°C. This fraction was redistilled retaining the distillate collected between 215°C and 217°C. After cooling in a dessicator containing Drierite, the distillate solidified as white needle-like crystals. In some preparations, liquid remained in the crystals and the mixture was then redistilled. The crystalline monohydrate (TFMSA) was stored under a nitrogen atmosphere in a closed container containing Drierite.

2. Gases

CP grade propane was obtained from Union Carbide Linde Division. Hydrogen gas was obtained from the Chemtron Corporation. House nitrogen (boil-off from liquid N_2) was also used in these experiments.

C. Platinum Coated IEM Electrode Assemblies

DuPont's unreinforced Nafion™ ion exchange membrane was

chosen as the basis of the ion exchange membrane electrode because it's fluorocarbon polymer structure is very similar to that of trifluoromethane-sulfonic acid. This ion exchange membrane also appeared to possess the chemical and thermal stability required for our purposes (6).

A method to produce a uniform conducting platinum surface on the IEM was developed at the General Electric Company (9). A search of current General Electric literature revealed that they produce a platinum coated Nafion^{TM} electrode (10) and a sample of PtIEM was obtained from the General Electric Company. This material was used in all the studies reported below.

The PtIEM electrode cell configuration shown in Figure 5 proved satisfactory for use in 85% H_3PO_4 solvent. The assembly of this electrode involved placing a 14 mm diameter PtIEM disk between the two (12 mm inside diameter) glass tubes using Goretex gaskets, as is shown in Figure 6. This assembly was then wrapped with 3 or 4 thicknesses of Teflon tape over which a sheath of polyethylene shrink tubing was placed, and then heat shrunk. Neither Goretex (a porous Teflon obtained from W. L. Gore & Assoc. Inc.), nor Teflon tape are wet by 85% H_3PO_4. The flattened end of a platinum wire that contacted the porous platinum was rigidly held between the PtIEM and upper Goretex gasket.

This assembly, shown in Figure 5, was used for initial studies in 85% H_3PO_4 and is referred to as the first electrode configuration.

In the TFMSA solvent, this electrode assembly usually leaked after several days use, because the solvent wet the Teflon tape and Goretex gasket. Also, at elevated temperature, a brown tint appeared in the TFMSA contacting the electrode. The source of this brown coloration was determined by individually placing each of the construction materials

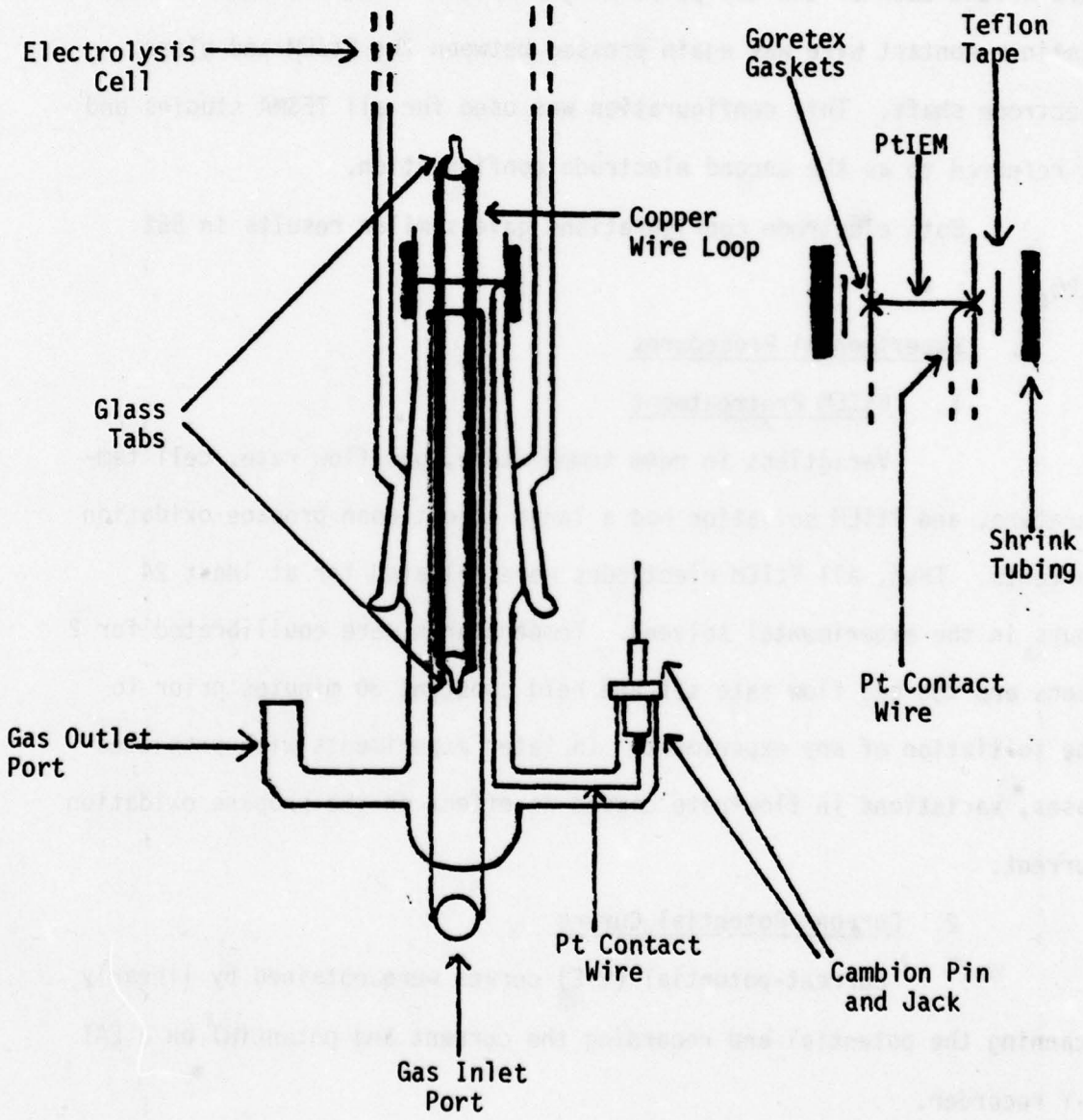

Figure 5. First Electrode Configuration

in fresh TFMSA at 140°C. The Teflon tape and polyethylene shrink tubing both discolored the solvent while the PtIEM left the TFMSA colorless.

A totally different electrode configuration was found necessary for use in TFMSA. The second electrode configuration developed used a 14 mm diameter PtIEM disk wedged in a 14/35 standard tapered glass joint as shown in Figure 6. The glass joint was secured by a loop of copper wire around each of the two pairs of glass tabs. The flat end of the platinum contact wire was again pressed between the PtIEM and glass electrode shaft. This configuration was used for all TFSMA studies and is referred to as the second electrode configuration.

Both electrode configurations gave similar results in 85% H_3PO_4.

D. Experimental Procedures

1. PtIEM Pretreatment

Variations in room temperature, gas flow rate, cell temperature, and PtIEM solvation had a large effect upon propane oxidation currents. Thus, all PtIEM electrodes were solvated for at least 24 hours in the experimental solvent. Temperatures were equilibrated for 2 hours and the gas flow rate set and held constant 30 minutes prior to the initiation of any experiment. In later experiments with preheated gases, variations in flow rate caused no effect on the propane oxidation current.

2. Current-Potential Curves

Current-potential (i-E) curves were obtained by linearly scanning the potential and recording the current and potential on a EAI X-Y recorder.

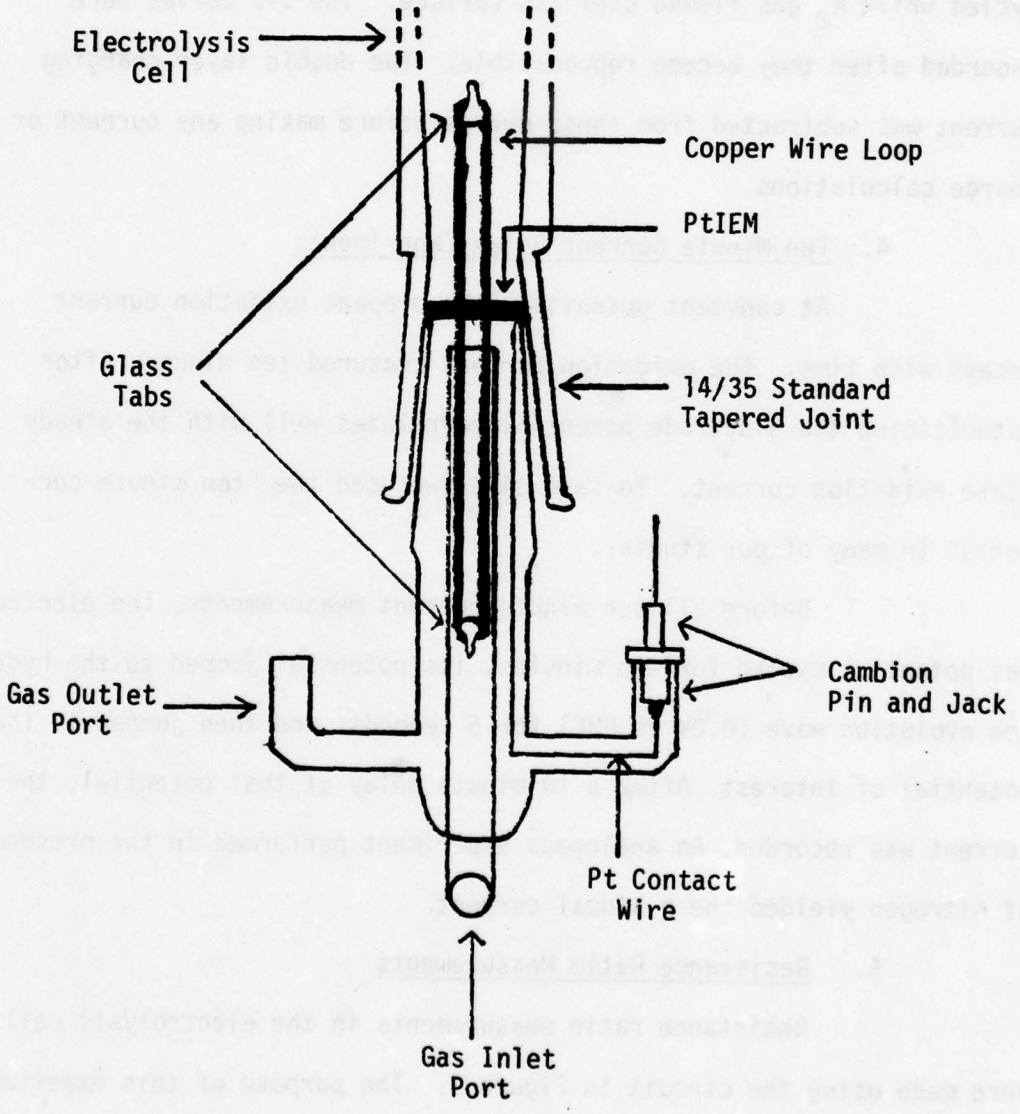

Figure 6. Second Electrode Configuration

3. Electrode Real Area Determinations

The geometric surface of each IEM disk was 1.54 cm^2. Each PtIEM electrode's real surface area was calculated from the total charge for the hydrogen desorption wave as indicated in the shaded portion of Figure 7, using the value of 210 μC of H_2 desorbed per real cm^2 of platinum (6). Surface roughnesses ranged from 20 to 100.

For all real area determinations, the electrode was potential cycled while N_2 gas flowed over its surface. The i-E curves were recorded after they became reproducible. The double layer charging current was subtracted from these curves before making any current or charge calculations.

4. Ten Minute Current Delay Experiments

At constant potential, the propane oxidation current decays with time. The oxidation current measured ten minutes after establishing the electrode potential correlates well with the steady state oxidation current. To save time, we used the "ten minute currents" in many of our studies.

Before all ten minute current measurements, the electrode was potential cycled for two minutes, its potential jumped to the hydrogen evolution wave (0.0V vs PHE) for 5 seconds, and then jumped to the potential of interest. After a 10 minute delay at that potential, the current was recorded. An analogous experiment performed in the presence of nitrogen yielded the residual current.

5. Resistance Ratio Measurements

Resistance ratio measurements in the electrolysis cell were made using the circuit in Figure 3. The purpose of this experiment was to determine the resistance ratio, R_R, given by Equation [1].

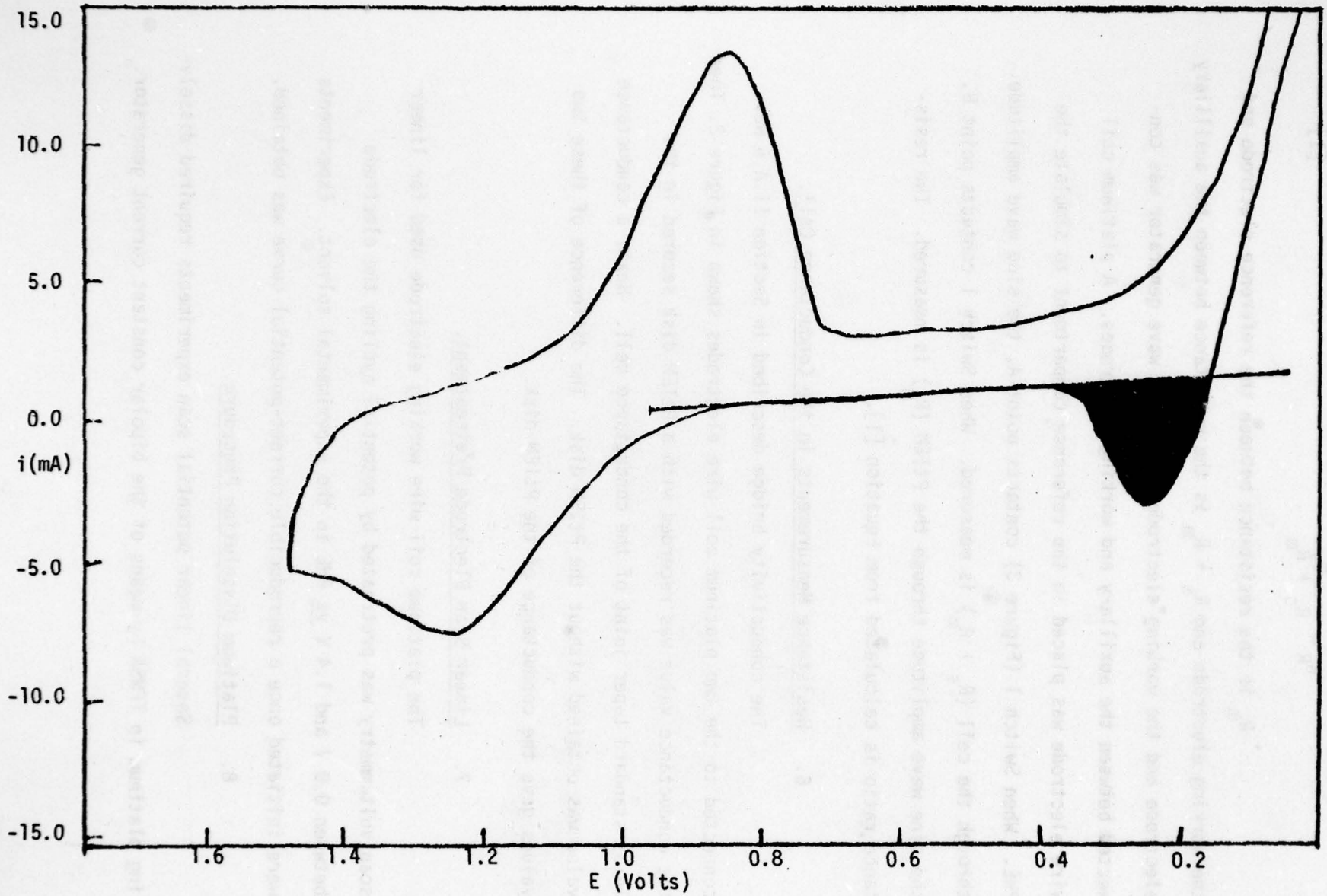

Figure 7. Electrode Real Area Determinations

$$R_R = \frac{R_m}{R_s + R_m} \qquad [1]$$

R_m is the resistance between the reference electrode and the working electrode and $R_s + R_m$ is the resistance between the auxilliary electrode and the working electrode. The sine wave generator was connected between the auxillary and working electrodes. A platinum coil wire electrode was placed in the reference compartment to simulate the PHE. When Switch 1 (Figure 3) contacts point A, the sine wave amplitude through the cell ($R_s + R_m$) is measured. When Switch 1 contacts point B, the sine wave amplitude through the PtIEM (R_m) is measured. The resistance ratio is calculated from Equation [1].

6. Resistance Measurements in the Conductance Cell.

The conductivity bridge described in Section II.A.6 was connected to the two platinum coil wire electrodes shown in Figure 2. Then the conductance value was recorded with a PtIEM disk secured in the 14/35 standard taper joint of the conductance cell. Next, a conductance value was obtained without the PtIEM disk. The difference of these two values gave the conductance of the PtIEM disk.

7. Linear Scan Electrode Pretreatment.

The platinum coil wire working electrode used for linear scan voltammetry was pretreated by potential cycling the electrode between 0.0 V and 1.4 V vs PHE in the experimental solvent. Experiments were initiated once a reproducible current-potential curve was obtained.

8. Platinum Dissolution Procedure.

Several linear potential scan experiments required dissolving platinum in TFMSA by means of the bipolar constant current generator.

This generator was connected between the auxilliary and working electrodes of the electrolysis cell and a 45 mA square wave current was passed for 30 minutes at 120°C. A black particulate material formed in the cell and there was darkening of the solvent. Experiments were then conducted in this darkened solvent and compared to those conducted in the same batch of solvent before platinum dissolution.

9. Potential Scanning Procedure

Current-potential curves at scan rates of 50, 100, and 200 mV/sec were recorded to differentiate between surface and non-surface processes. The working electrode was potential cycled at each scan rate until a reproducible i-E curve could be recorded.

10. Consecutive Potential Scanning Procedure.

The consecutive potential scan procedure consisted of two separate steps. First, the working electrode potential was set to the value of interest for a predetermined period of time. Then the electrode potential was jumped to zero volts vs the PHE and scanned immediately in an anodic direction to the anodic limit. Three consecutive cyclic potential scans were then recorded, and are so numbered on the figures referenced.

E. Factorial Data Analysis

Factorial experiment data were analyzed as described by Davis (7). The analysis of the three variables' effect upon propane electro-oxidation was performed at both the quadratic and linear levels. From each factorial data set, a prediction equation was calculated. This equation estimates at the 95% confidence level the response for any set of variable values within the original variable ranges.

CHAPTER III

ELECTROCATALYTIC BEHAVIOR OF PtIEM ELECTRODES

A. Initial Current-Potential Comparisons

Current-potential curves were recorded using both 85% H_3PO_4 and TFMSA as solvents in the presence of one atmosphere of propane or nitrogen. Figure 8 shows the current-potential curve of propane electrooxidation at a PtIEM electrode solvated in 85% H_3PO_4 ($PtIEM_{H_3PO_4}$) at 120°C and 135°C. The large effect on the anodic current caused by this 15°C temperature difference agrees with previous observations in 85% H_3PO_4 using conventional Teflon bonded platinum structures (1,2).

The current-potential curve obtained at a PtIEM electrode solvated in TFMSA ($PtIEM_{TFMSA}$) at 120°C is shown in Figure 9. The slope and lack of definition of the i-E curve in Figure 9 suggests there is a large IR drop in the $PtIEM_{TFMSA}$ electrode. This matter is examined in a later section.

The Ten Minute Current Density (TMCD) vs E curves recorded in both 85% H_3PO_4 and TFMSA at 120°C are shown in Figure 10. The peak propane electrooxidation current density recorded with a $PtIEM_{TFMSA}$ electrode was 1.8 times that recorded with a PtIEM H_3PO_4 electrode. These propane oxidation peak current densities were at least ten times the peak currents reported with a platinum wire mesh electrode.

Propane oxidation in TFMSA occurs over a much wider potential range, from 0.2V to 1.8V, than in 85% H_3PO_4. from 0.9 V to 1.1 V.

An anodic current for propane oxidation only 1.8 times greater in TFMSA than in 85% H_3PO_4 is less than what was anticipated.

These initial results seemed promising and it was felt worthwhile to try to identify the variables that influence propane oxidation at PtIEM electrodes.

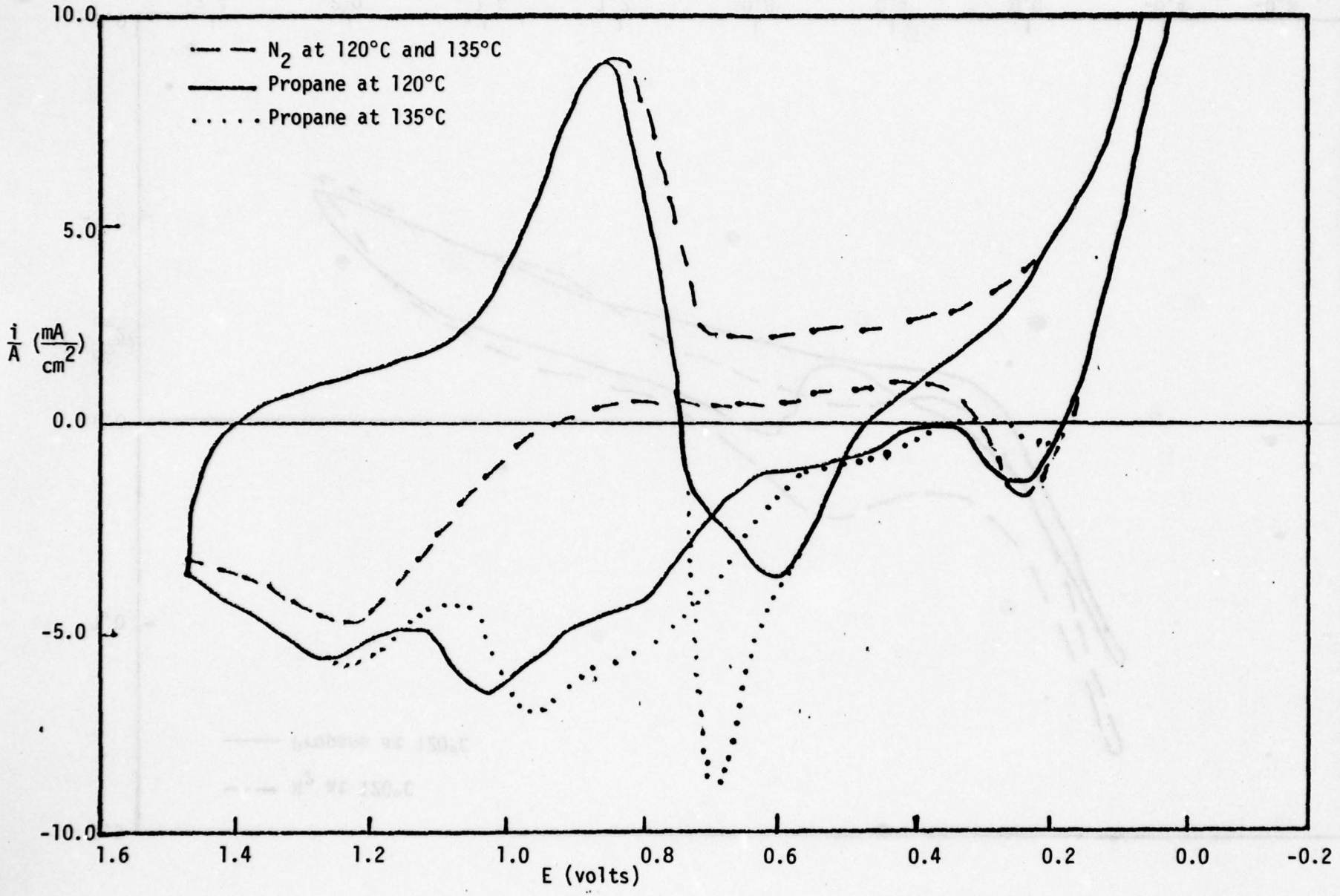

Figure 8. Propane Oxidation on a PtIEM H_3PO_4 Electrode

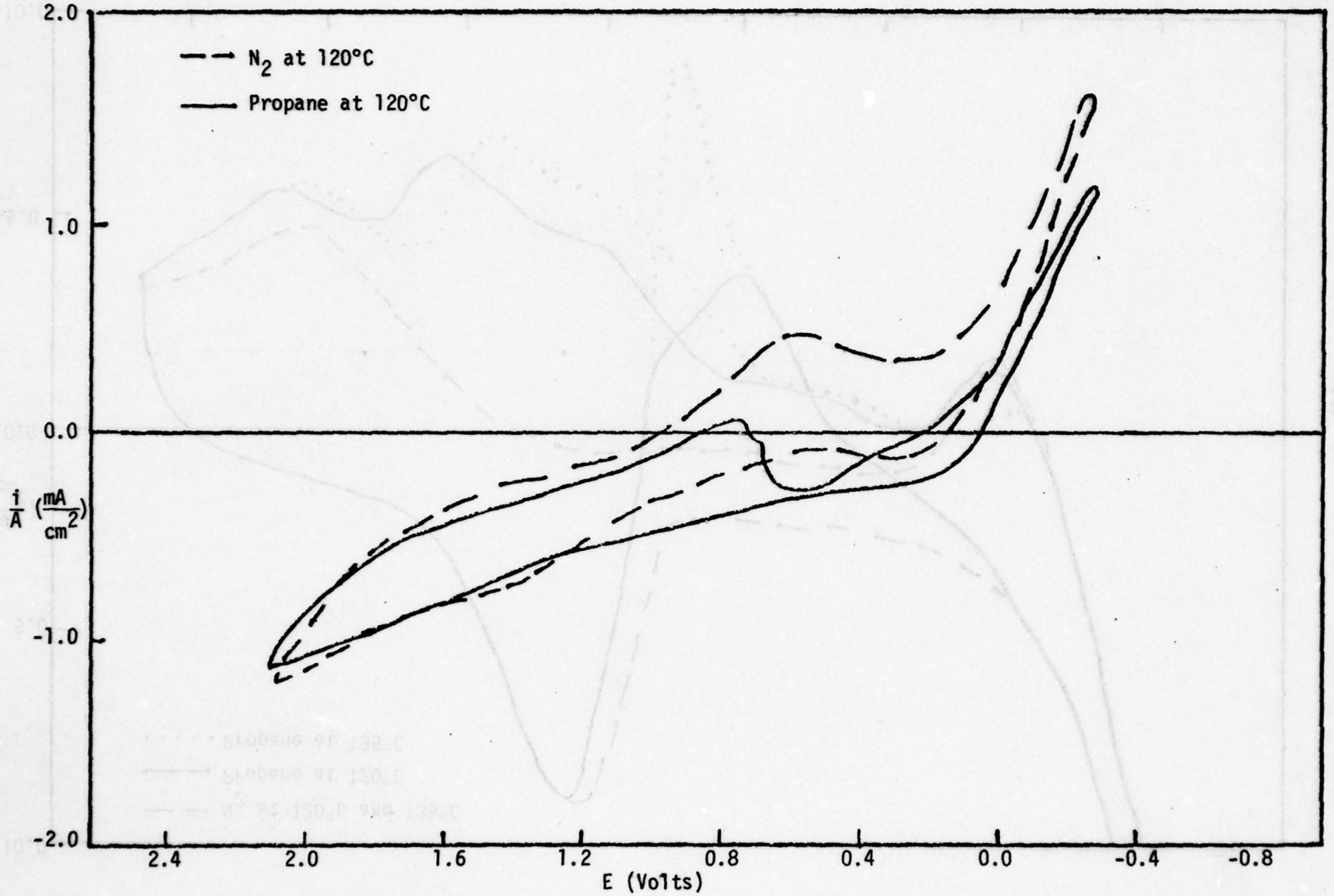

Figure 9. Propane Oxidation on a $PtIEM_{TFMSA}$ Electrode

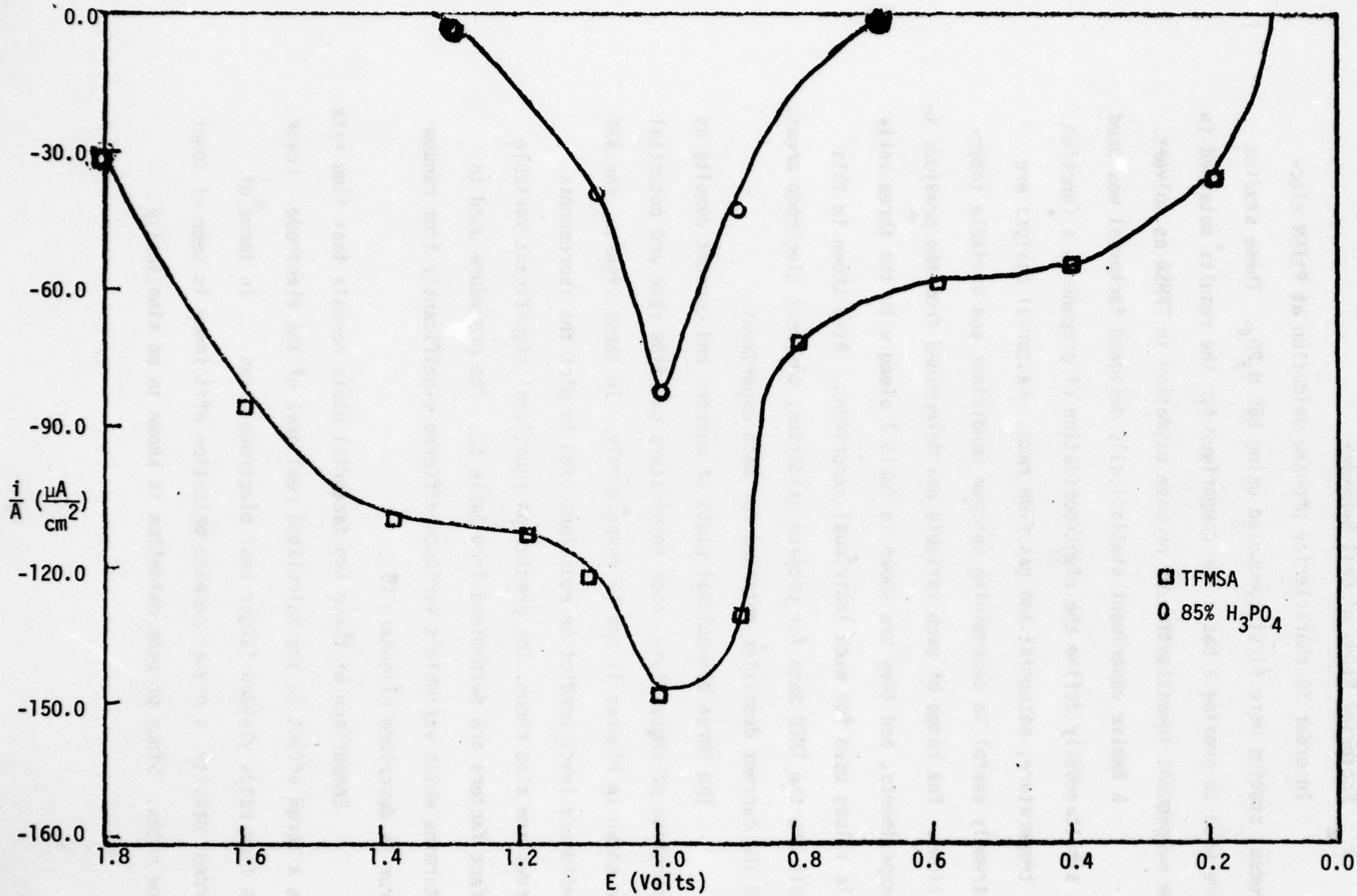

Figure 10. Propane Oxidation Current After 10 Minutes

B. Factorial Study of Cell Behavior

In order to characterize propane oxidation at PtIEM electrodes, studies were first conducted using 85% H_3PO_4. These studies were used to provide a basis for comparison for the results obtained in the subsequent investigation of propane oxidation in TFMSA as solvent.

A twelve experiment statistically designed factorial was used to simultaneously define the electrooxidation of propane as a function of temperature, potential and gas flow rate. Factorial designs are extremely useful in determining optimum conditions and variable interactions. The range of each variable was determined from the previous i-E experiments, and they are shown in Table I along with the three variable values used for each individual experiment. Also shown in this table are the TMCD data for propane oxidation, the real electrode areas, and the current densities obtained for each experiment.

The three dimensional plots of current and current density as a function of temperature, room temperature gas flow rate and potential are shown in Figures 11 and 12 respectively. In these figures, the 95% confidence level prediction equations used to plot the isoresponse curves are also shown. The prediction equations' significant variable effect factors are determined from Table II. The procedure used to determine which variable's variance differed significantly from random error is described elsewhere (7).

Comparison of these two factorial plots reveals that flow rate has a large effect on the calculated real area of the electrode. Lower gas flow rates yielded larger real electrode areas. In terms of current density, a higher propane oxidation efficiency is seen at lower flow rates. Since propane oxidation is known to be kinetically

TABLE I

FACTORIAL EXPERIMENT

Non-Preheated Gases

RUN #	Expt. #	X_T	X_F	X_E	i(mA)	area (cm^2)	$\frac{i}{A}$ ($\frac{\mu A}{cm^2}$)
1	3	+	+	0	5.57	52.4	106.3
2	2,8	+	+	-	2.90, 2.74	58.3, 59.5	50.7, 46.1
3	11	+	-	0	6.31	84.5	74.7
4	9	+	-	-	3.99	86.9	45.9
5	4	-	+	0	2.72	65.5	41.5
6	6	-	+	-	1.22	63.1	19.3
7	1	-	-	0	4.12	151.2	27.2
8	5,7	-	-	-	1.72, 1.63	95.2, 109.5	18.1, 14.9
9	12	-	+	+	2.40	59.2	40.5
10	13	-	-	+	2.59	90.5	28.6
11	14	+	+	+	5.57	50.0	111.4
12	15	+	-	+	4.45	133.3	33.4
			average		3.62	83.2	49.5

	VARIABLE RANGES			
	-	0	+	
Temperature	120		135	°C
Flow Rate	0.01		0.21	ℓ/min
Potential	0.90	1.00	1.10	Volts

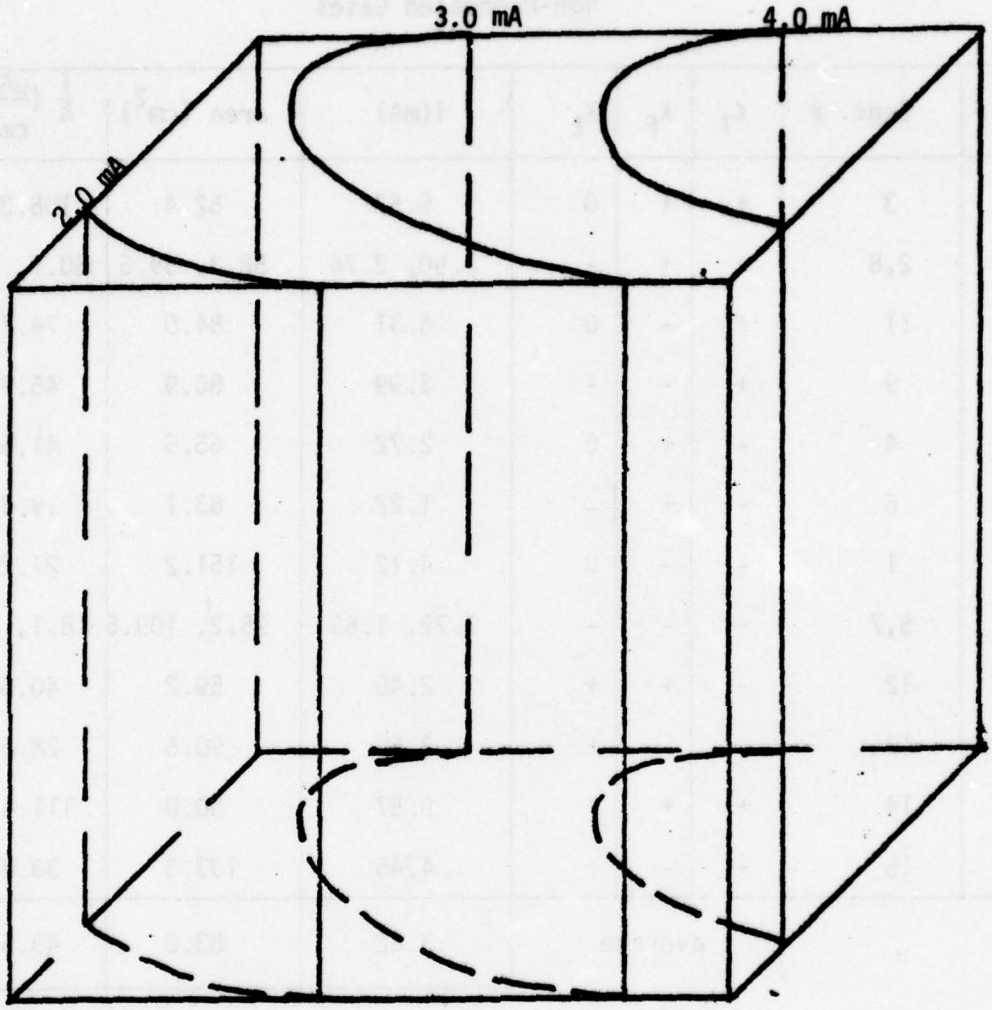

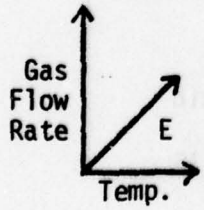

$$i = 3.62 + 1.17\ X_T + 0.66\ X_E - 0.80\ X_E^2$$

Figure 11. First Factorial Three Dimensional Current Plot

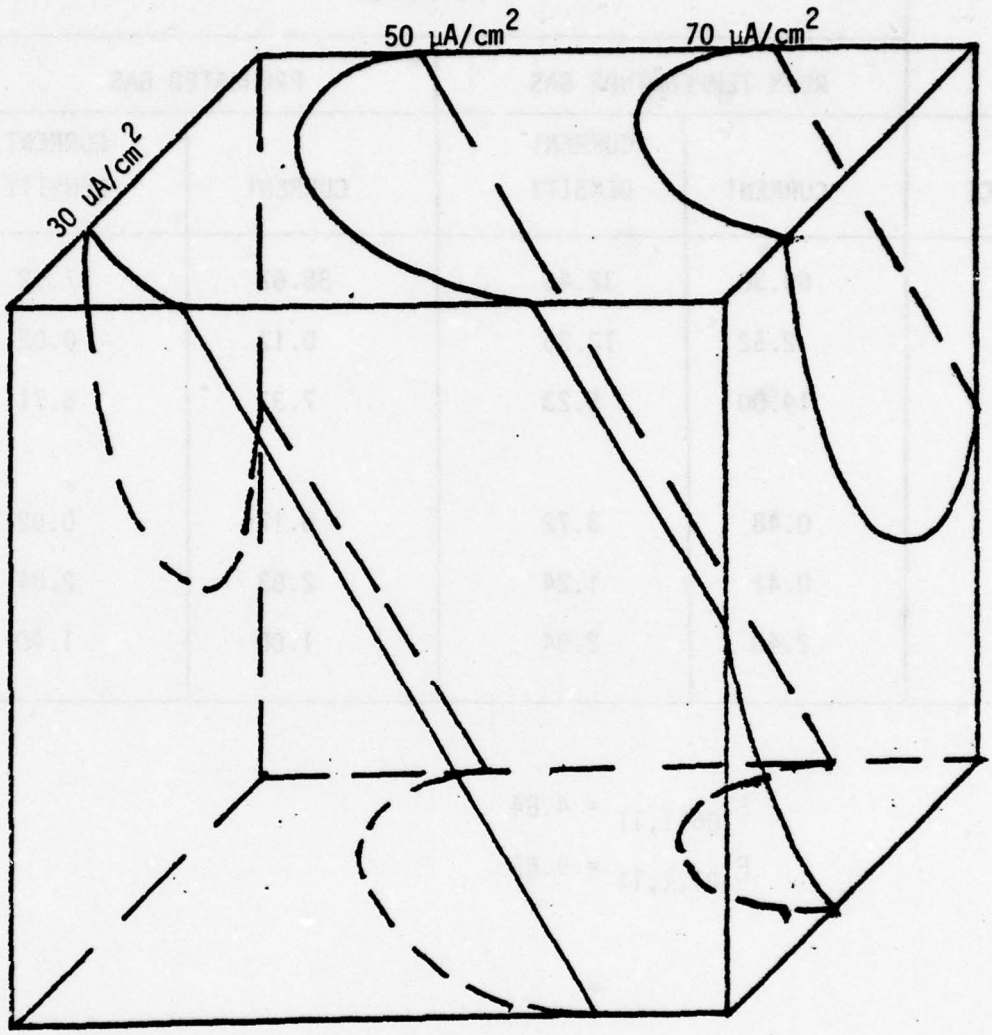

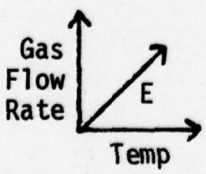

$$i/A_r = 49.5 + 20.4\ X_T + 11.6\ X_f + 10.4\ X_E - 9.8\ X_E^2$$

Figure 12. First Factorial Three Dimensional Current Density Plot

TABLE II

ANALYSIS OF VARIANCE FOR FIRST AND SECOND FACTORIAL

	FACTORIAL			
	ROOM TEMPERATURE GAS		PREHEATED GAS	
SOURCE	CURRENT	CURRENT DENSITY	CURRENT	CURRENT DENSITY
X_T	60.30	32.48	35.67	37.52
X_F	2.52	12.26	0.17	0.02
X_E	19.00	5.23	7.33	5.71
X_{Tf}	0.48	3.72	0.17	0.02
X_{TE}	0.41	1.24	2.83	2.84
X_{fE}	2.48	2.94	1.00	1.40

$F_{.05,1,11} = 4.84$

$F_{.01,1,11} = 9.65$

controlled (1,2), the observed flow rate effect is inconsistent with the previous result. The cause of this flow rate effect is shown below to be due to the cooling of the IEM by the flow of room temperature gas over its surface.

A second factorial set of experiments using the same variable ranges as in the first factorial was done with preheated gases. The results are presented in Table III. Figures 13 and 14 show current and current density, respectively, plotted in three dimensions as a function of temperature, preheated gas flow rate, and potential. The propane current density's dependence upon flow rate no longer exists, as seen in Table III. Propane electrooxidation current density is dependent only upon temperature and potential, as was the case in the systems studied by previous workers using 85% H_3PO_4.

Initial studies in TFMSA with preheated propane show effects similar to those in Figure 13 with respect to flow rate, temperature, and potential. Reliable real area determinations at the $PtIEM_{TFMSA}$ electrode were impossible because of the inherent slope of the i-E curve, as seen in Figure 9.

C. Steady State Electrooxidation Experiments

Preheated propane, nitrogen, and a 9% hydrogen-nitrogen gas mixture were successively passed over a PtIEM electrode in both TFMSA and 85% H_3PO_4 and the steady state currents determined at constant E. The same PtIEM electrode was used with both solvents to eliminate any variation resulting from estimates of the electrode's geometric area.

TABLE III

FACTORIAL EXPERIMENT

Preheated Gases

Run #	Expt. #	X_T	X_F	X_E	i(mA)	area (cm^2)	$\frac{i}{A}$ ($\frac{\mu A}{cm^2}$)
1	4	+	+	+	1.97	24.3	81.1
2	3	+	+	0	2.11	25.1	84.1
3	8	+	-	+	1.39	24.5	56.7
4	6	+	-	0	2.43	21.3	114.1
5	2	-	+	+	0.70	28.1	24.9
6	7	-	+	0	1.16	34.1	34.0
7	5	-	-	+	0.64	31.8	20.1
8	1	-	-	0	1.08	31.6	34.2
9	9	+	+	-	1.31	27.2	48.2
10	10	+	-	-	1.24	25.3	49.0
11	12	-	+	-	0.80	33.7	23.7
12	11	-	-	-	1.00	35.2	28.4
				average	1.32	28.5	49.9

	VARIABLE RANGES			
	-	0	+	
Temperature	120		135	°C
Flow Rate	0.01		0.21	ℓ/min
Potential	0.90	1.00	1.10	VOLTS

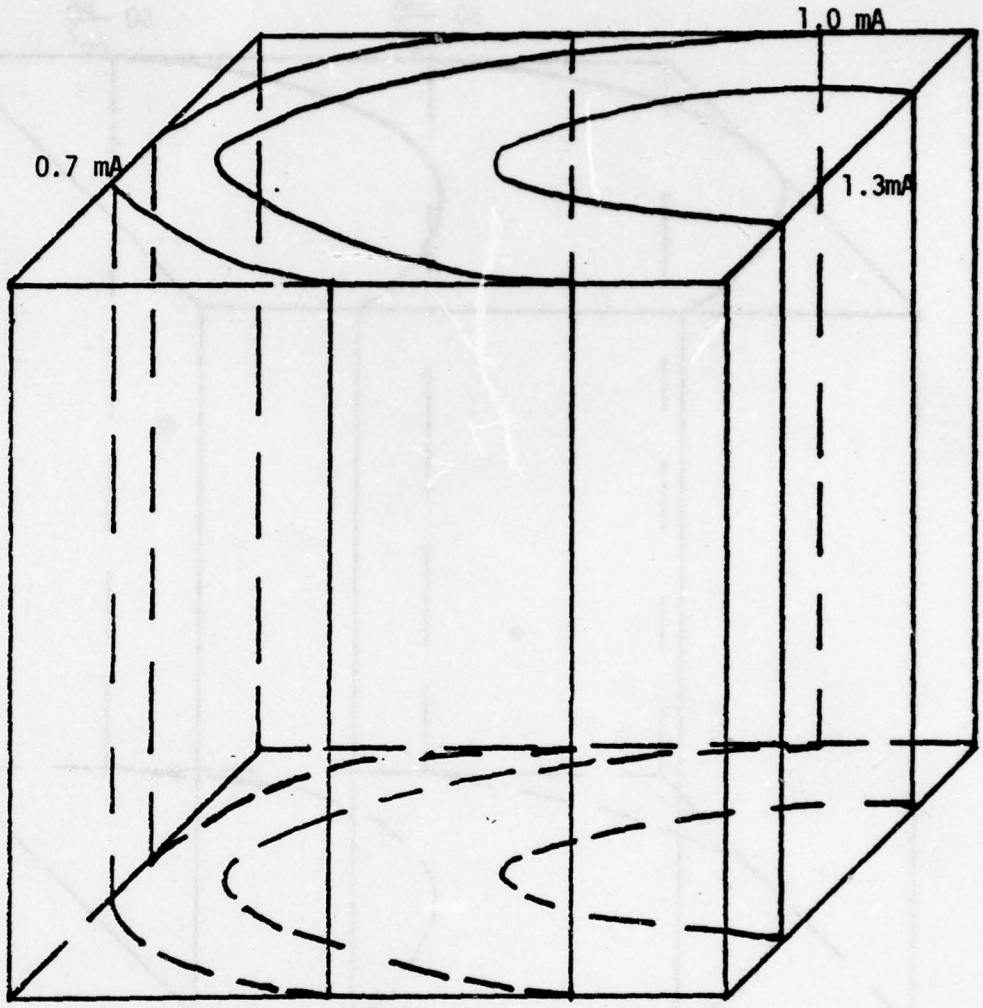

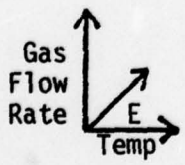

$$i = 1.32 + 0.43\ X_T - 0.57\ X_E^2$$

Figure 13. Second Factorial Three Dimensional Current Plot

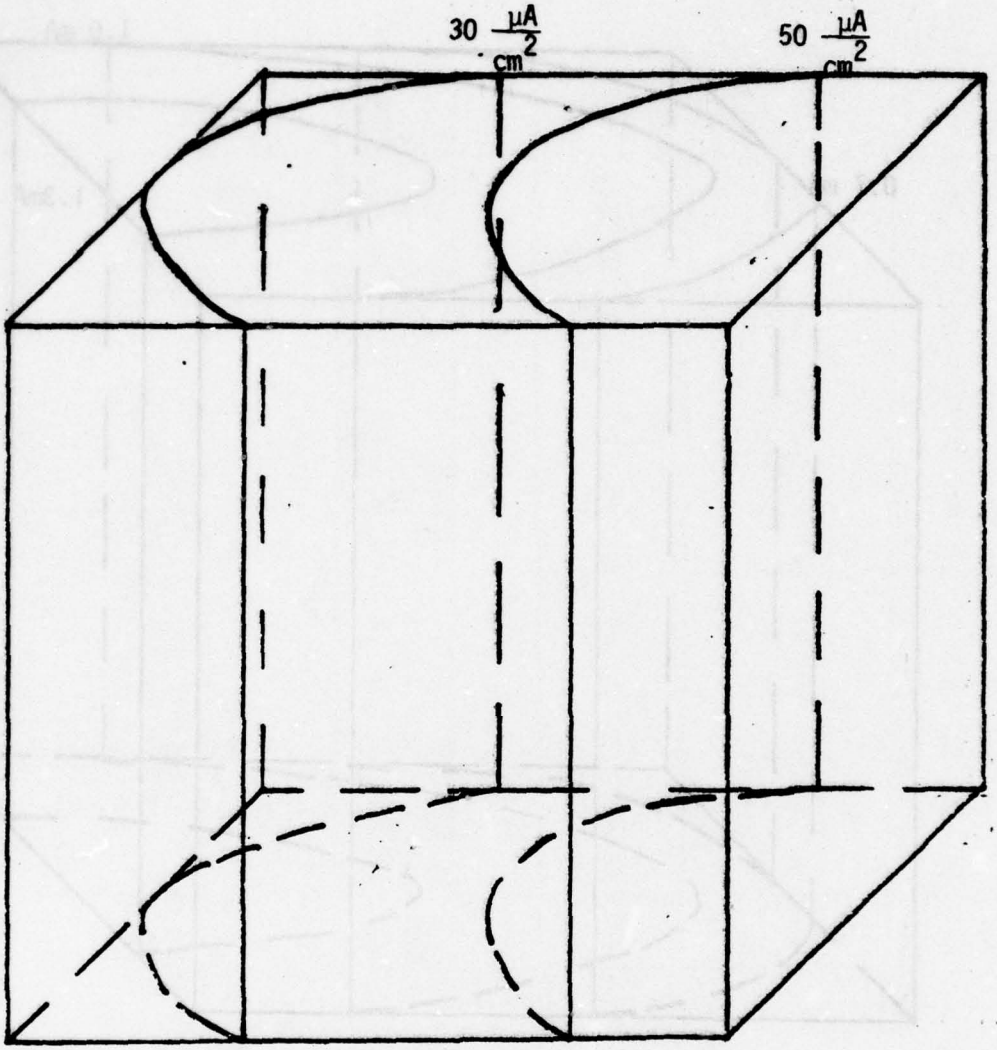

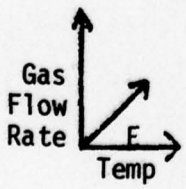

$$i/A_r = 49.9 + 22.3\ X_T - 12.5\ X_E^2$$

Figure 14. Second Factorial Three Dimensional Curent Density Plot

A PtIEM electrode which had been used in previous experiments was used in the first set of steady state experiments. In this study the temperature was maintained at 120°C with a preheated gas flow rate of 0.11 l/min and a constant potential of 0.90 V vs. the PHE. The results of these steady state experiments are shown in Table IV.

All currents reported as steady state remained within the ranges reported for at least 2 hours. The absolute value for propane steady state currents with the $PtIEM_{H_3PO_4}$ electrode was 21.9 μA compared to 66.9 μA for the $PtIEM_{TFMSA}$ electrode. Repeating these experiments several times gave similar results. The values reported indicate a propane oxidation current increase of three fold for TFMSA as compared to 85% H_3PO_4. This result agrees with that expected from Figure 10.

Steady state current values for 9% hydrogen-nitrogen mixture and propane were also determined with a fresh PtIEM electrode in TFMSA and 85% H_3PO_4. These experiments were carried out in the same manner as above. All these experiments were done at a flow rate of 0.11 l/min, a temperature of 120°C, and a potential of 1.0 V vs. PHE on the same PtIEM disk. As shown in Table V, the propane current produced by the $PtIEM_{TFMSA}$ electrode was twice that produced by the $PtIEM_{H_3PO_4}$ electrode. This current ratio again agrees with that predicted by Figure 10. For the 9% hydrogen-nitrogen gas mixture, the $PtIEM_{TFMSA}$ electrode produced 0.8 times the anodic current of the $PtIEM_{H_3PO_4}$ electrode. This result is contrary to previous literature for which an enhanced hydrogen current was found in TFMSA as compared to 85% H_3PO_4 with a platinum mesh electrode system (2).

This result indicates that the PtIEM electrode electrooxidizes hydrogen equally well when saturated with either 85% H_3PO_4 or TFMSA, and

TABLE IV

STEADY STATE CURRENTS AT AN AGED PtIEM ELECTRODE				
SOLVENT	GAS	EXPT. DURATION	STEADY STATE CURRENT	DURATION AT STEADY STATE CURRENT
85% H_3PO_4	N_2	307 min.	$+1.5 \pm 0.5$ μA	205 min.
	Propane	248 min.	-20.4 ± 0.5 μA	180 min.
TFMSA	N_2	590 min	$+5.0 \pm 0.8$ μA	280 min.
	Propane	222 min.	-61.9 ± 0.8 μA	130 min.

TABLE V

STEADY STATE CURRENTS AT A FRESH PtIEM ELECTRODE

	Electrode	
GAS	$PtIEM_{H_3PO_4}$	$PtIEM_{TFMSA}$
Propane	0.83 mA	1.68 mA
9% Hydrogen	21.9 mA	18.7 mA
Nitrogen	0.0 mA	0.0 mA

oxidation is probably proceeding at a mass transfer or cell geometry controlled rate.

The 9% hydrogen gas steady state current on the $PtIEM_{H_3PO_4}$ electrode was thirteen times the anodic current produced with propane gas on the $PtIEM_{TFMSA}$ electrode. The anodic current per geometric area per mole of oxidizable gas was approximately 145 times greater for hydrogen as compared to propane at this flow rate. This result indicates that the improvement in the electrooxidation of propane at a PtIEM electrode in going from 85% H_3PO_4 to TFMSA as solvent is not really very large. The current efficiency for propane oxidation remains small compared to that of hydrogen oxidation.

Comparing the steady state propane oxidation values found at the fresh $PtIEM_{TFSMA}$ electrode with those found at the used $PtIEM_{TFMSA}$ electrode shows that the fresh $PtIEM_{TFMSA}$ electrode gives about twenty-two times larger a current density than at a used PtIEM electrode.

D. Solvent and PtIEM Conductance Measurements

Because of the large slope observed in all i-E curves recorded at a $PtIEM_{TFMSA}$ electrode, a study of resistances in the electrolysis cell was undertaken.

The resistance in the electrolysis cell was determined using the AC conductance bridge. The AC bridge was connected between the working and auxilliary electrodes while in the same configuration as used to obtain all previous i-E curves. The measured resistance at 120°C was 60 ohms with 85% H_3PO_4 compared to 540 ohms with TFMSA solvent. Therefore, the resistance in this electrolysis cell is nine times greater with TFMSA then with 85% H_3PO_4 using the same PtIEM disk.

Using the circuit shown in Figure 3A, a resistance Ratio (R_R) of approximately 0.8 was calculated with a $PtIEM_{H_3PO_4}$ electrode at 120°C.

Therefore, 80% of the electrolysis cell's total resistance was the resistance through the PtIEM electrode.

Since the resistance through the PtIEM in the electrolysis cell was so large, resistance measurements of the PtIEM disks in TFMSA and 85% H_3PO_4 were necessary. The conductance cell was used for this purpose. Two fresh 14 mm diameter PtIEM disks were each exposed only to one of the solvents. The resistance for the $PtIEM_{H_3PO_4}$ disk and the 85% H_3PO_4 filled cell was measured to be 27.0 $\pm$ 0.5 ohms while the resistance for 85% H_3PO_4 filled cell without the $PtIEM_{H_3PO_4}$ disk was 25.0 $\pm$ 0.5 ohms. The resistance through the $PtIEM_{H_3PO_4}$ disk was, therefore, $\sim$2.0 ohms. The $PtIEM_{TFMSA}$ disk resistance was measured to be $\sim$20 ohms since the cell resistance with the solvent was 170 $\pm$ 5 ohms and the cell resistance solvent plus $PtIEM_{TFMSA}$ disk was 190 $\pm$ 5 ohms. The $PtIEM_{TFMSA}$ disk, therefore, has a resistance of approximately ten times the resistance of $PtIEM_{H_3PO_4}$ disk. This value agrees with the nine fold increase found in the electrolysis cell.

Since the electrolysis cell with the used $PtIEM_{H_3PO_4}$ disk gave a total resistance of 60 ohms and the resistance ratio was calculated to be 0.80, the resistance through the $PtIEM_{H_3PO_4}$ disk was 48 ohms. The measured resistance through a fresh $PtIEM_{H_3PO_4}$ disk was two ohms. This difference in resistance is due to the amount of use each PtIEM electrode underwent. The used $PtIEM_{H_3PO_4}$ electrode's resistance was 24 times that of the fresh $PtIEM_{H_3PO_4}$ electrode. This resistance ratio value is similar to the ratio of propane steady state oxidation currents on a fresh $PtIEM_{TFMSA}$ electrode and on the used $PtIEM_{TFMSA}$ electrode (twenty-two). This result strongly suggests that propane oxidation currents at the PtIEM electrode become resistance limited as the IEM ages.

CHAPTER IV

DISSOLUTION OF PLATINUM IN TFMSA

A. Qualitative identification of Platinum

While experiments were being conducted in the electrolysis cell with TFMSA solvent, a black precipitate rapidly formed in the reference and auxilliary compartments. This phenomena was not observed with 85% H_3PO_4 under the same conditions. The black precipitate was isolated and analyzed.

The precipitate proved to be insoluble in both concentrated HNO_3 and concentrated HCl, but dissolved in aqua regia. This suggested that the precipitate was platinum. The $SnCl_2$ test for platinum was used as the confirming test, as described elsewhere (11).

When $SnCl_2$ was added to an aqua regia solution of the black precipitate, an orange colored solution resulted. A platinum wire dissolved in aqua regia and tested with $SnCl_2$ also gave an orange solution. The blank, $SnCl_2$ and pure aqua regia, produced a colorless solution. These tests confirm that the black precipitate contained large amounts of platinum.

B. Electrochemical Conditions for Platinum Dissolution

The conditions needed for platinum dissolution and precipitation in TFMSA were next determined. Two platinum coil wire electrodes connected to a square wave current generator ($\pm$ 45 mA) were immersed in TFMSA. No change was visible at room temperature, but the black precipitate formed rapidly at 120°C. This precipitate was isolated and also gave a positive $SnCl_2$ test for platinum.

Two gold coil wire electrodes were then immersed in the used TFMSA. When current was passed through the electrodes black precipitate again appeared. Current passed through these same gold electrodes in

fresh TFMSA at 120°C resulted in production of a brown precipitate not a black precipitate.

A study of the platinum dissolution in TFMSA with linear scan voltammetry was next used in an attempt to understand the above phenomenon. Linear scan experiments at a platinum wire electrode were conducted in the same electrolysis cell used with the PtIEM electrode to make comparison easy between i-E curves previously obtained. Compare the dashed i-E curve in Figure 9, which was obtained in TFMSA with a PtIEM electrode, to the solid i-E curve in Figure 15, which was obtained in TFMSA with the platinum working electrode. The potential scan rates were 40 mv/sec for the PtIEM electrode and 100 mv/sec with the wire electrode. The i-E curves obtained with the $PtIEM_{TFMSA}$ electrode have a large slope as compared to the platinum wire electrode. These i-E curves are further proof of the $PtIEM_{TFMSA}$ electrode's high resistance.

The effect of time on the i-E curves obtained with the linear scan working electrode are shown in Figure 15. The dashed curve was recorded in fresh TFMSA while the solid curve was recorded 12 hours later. There was no current flow between the working and auxilliary electrodes in the time interval between recording these two current-potential curves. The solid curve resembles i-E curves recorded by previous workers at a rotating disk electrode (12). The reason for this change of the i-E curves with time is not understood. Apparently a reducible species has vanished.

Platinum was caused to dissolve in two separate samples of TFMSA corresponding to the solutions that yielded one or the other of the i-E curves given in Figure 15. The resulting i-E plots are shown

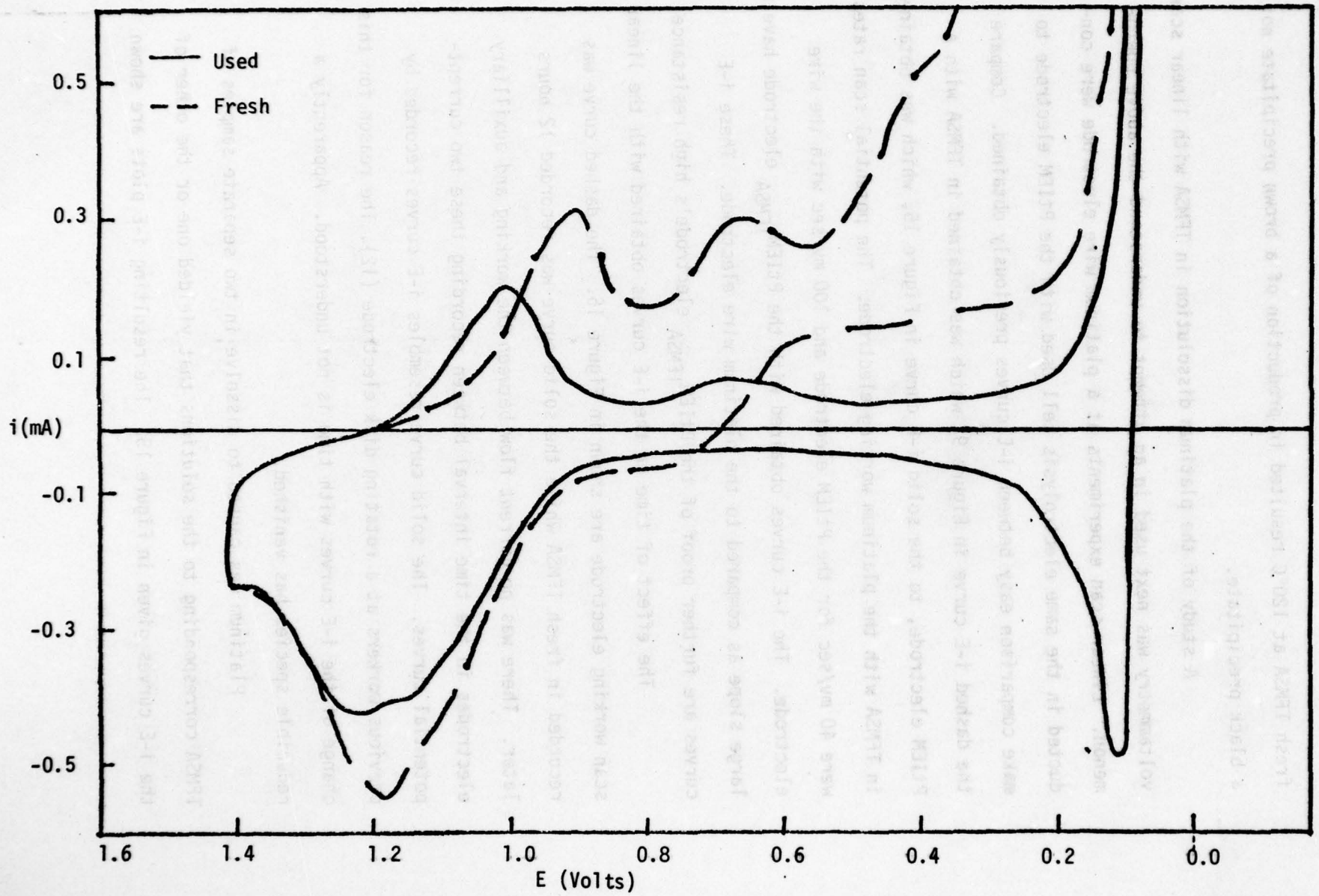

Figure 15. Current-Potential Curves of Fresh and Used TFMSA.

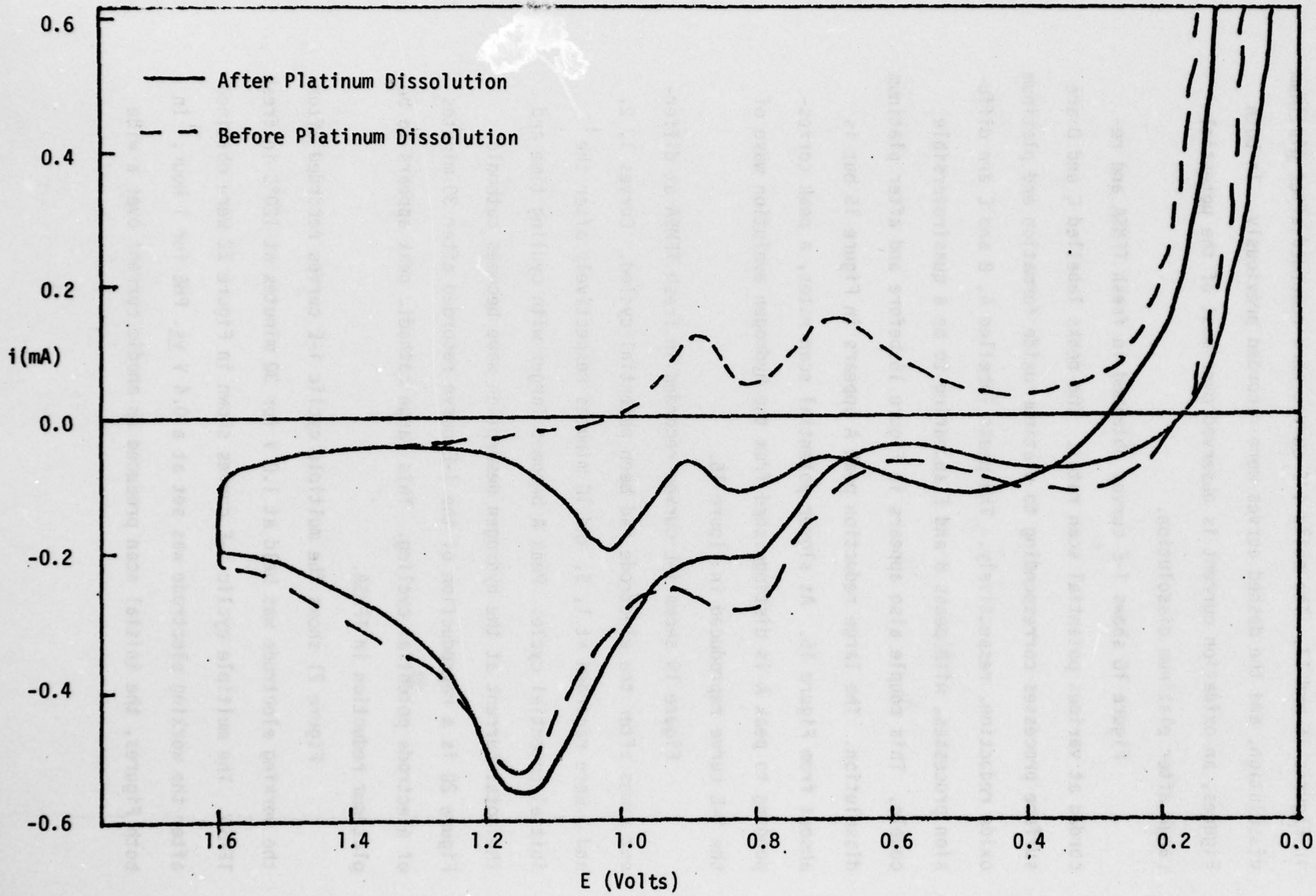

Figure 16. Current-Potential Curves Before and After Platinum Dissolution in New TFMSA

in Figures 16 and 17. The solid i-E curves were recorded after platinum dissolution, and the dashed curves were recorded previously. In both Figures, an oxidation current is observed over most of the potential range after platinum dissolution.

Figure 18 shows i-E curves obtained in fresh TFMSA and recorded at various potential scan rates. The peaks labelled C and D are surface processes corresponding to platinum oxide formation and platinum oxide reduction, respectively. The peaks labelled A, B and E are diffusion processes, with peaks B and E appearing to be a quasireversible couple. This couple also appears in Figure 16 before and after platinum dissolution. The large reduction peak A appears in Figure 15 but is absent from Figure 16. At slower potential scan rates, a peak corresponding to peak A is distinguished from the hydrogen evolution wave of the i-E curve reproduced in Figure 16.

Figure 19 shows i-E curves recorded in fresh TFMSA at different times after the electrode had been potential cycled. Curves 1, 2, and 3 were recorded at 1, 5, and 10 minutes respectively after the initial potential cycle. Peak A becomes larger with cycling time and the total current at the hydrogen desorption wave becomes cathodic. Figure 20 is a reproduction of the i-E curve recorded after 30 minutes of electrode potential cycling. This large cathodic peak appears to be platinum reduction in TFMSA.

Figure 21 shows the multiple cyclic i-E curves recorded after the working electrode was held at 1.0 V for 30 minutes at 120°C in fresh TFMSA. The multiple cyclic i-E curves shown in Figure 22 were obtained after the working electrode was set at a 0.4 V vs. PHE for 1 hour. In both Figures, the initial scan produced an anodic current over a wide

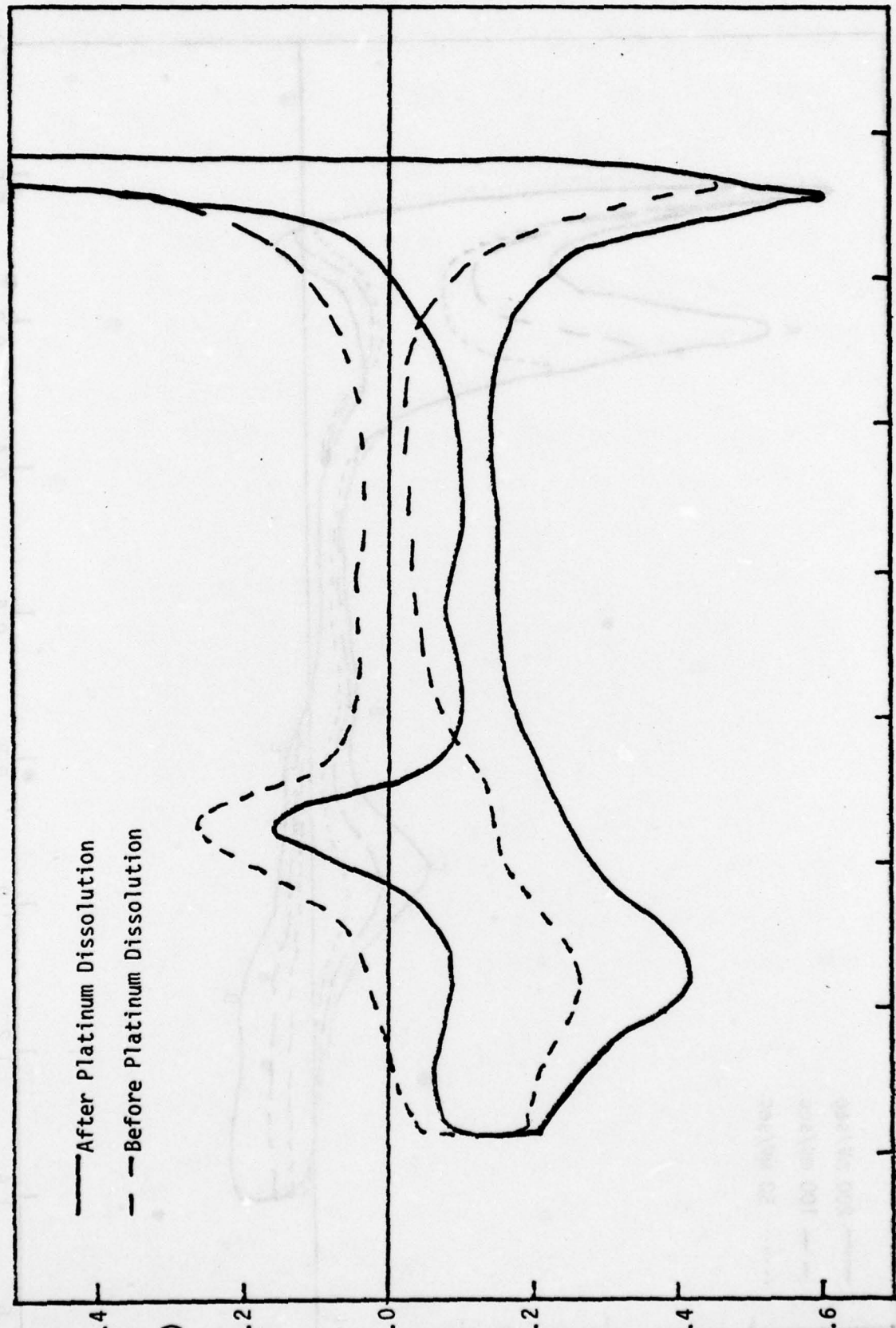

Figure 17. Current-Potential Curves Before and After Platinum Dissolution in Used TFMSA

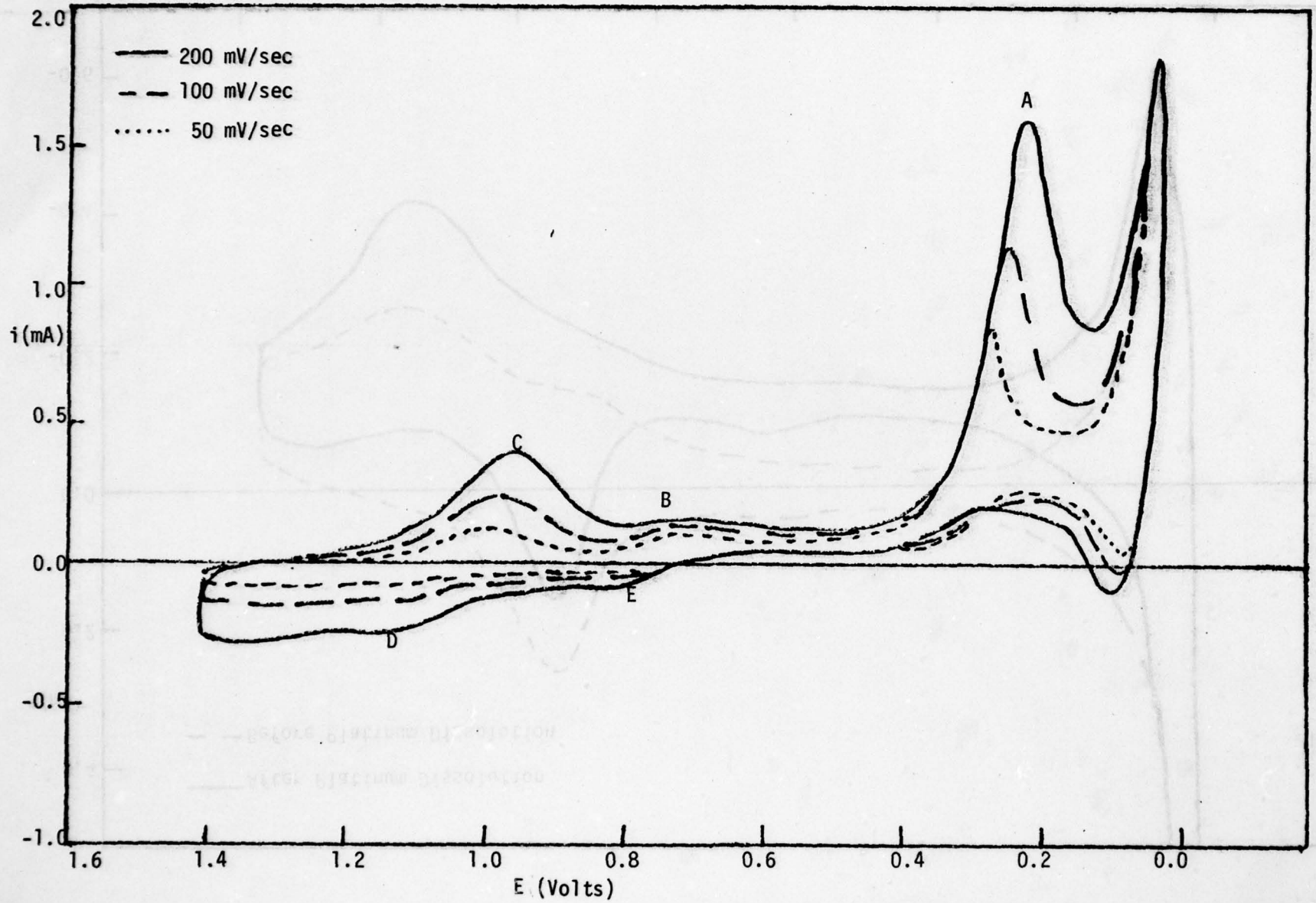

Figure 18. Current-Potential Curve in Fresh TFMSA - Effect of Potential Scan Rate

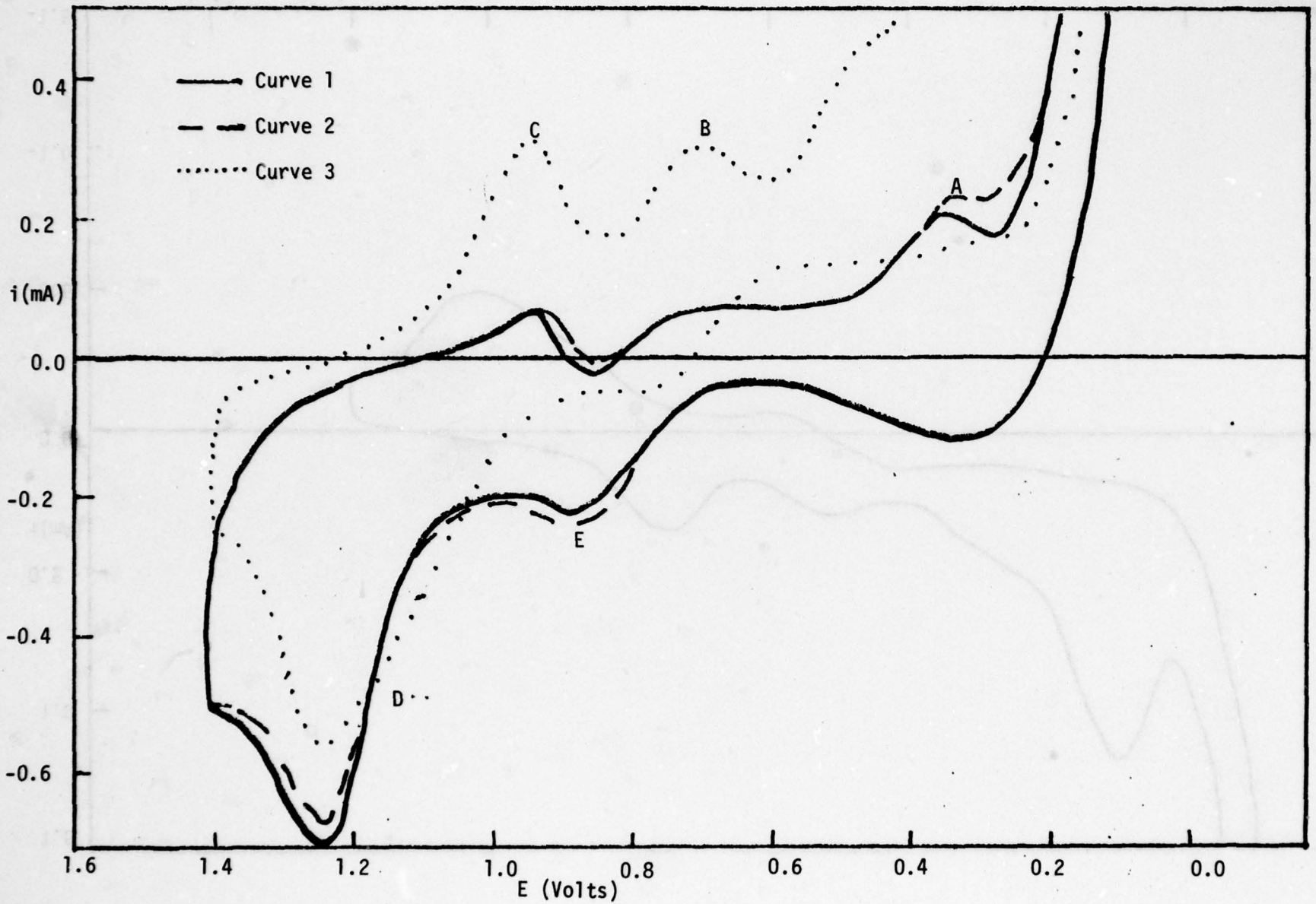

Figure 19. Current-Potential Curves in Fresh TFMSA - Effect of Time

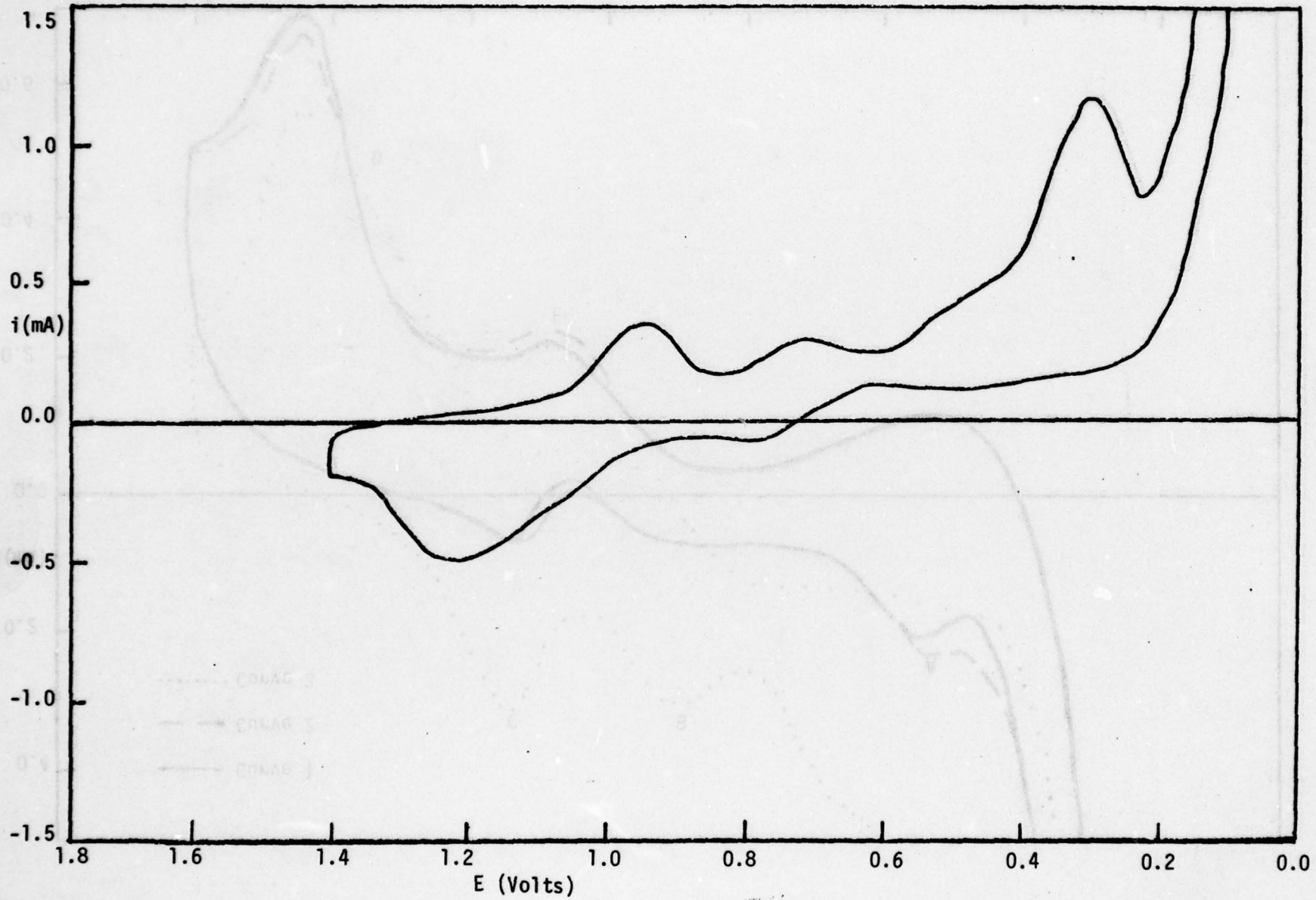

Figure 20. TFMSA Current-Potential Curve After 30 Minutes of Potential Cycling

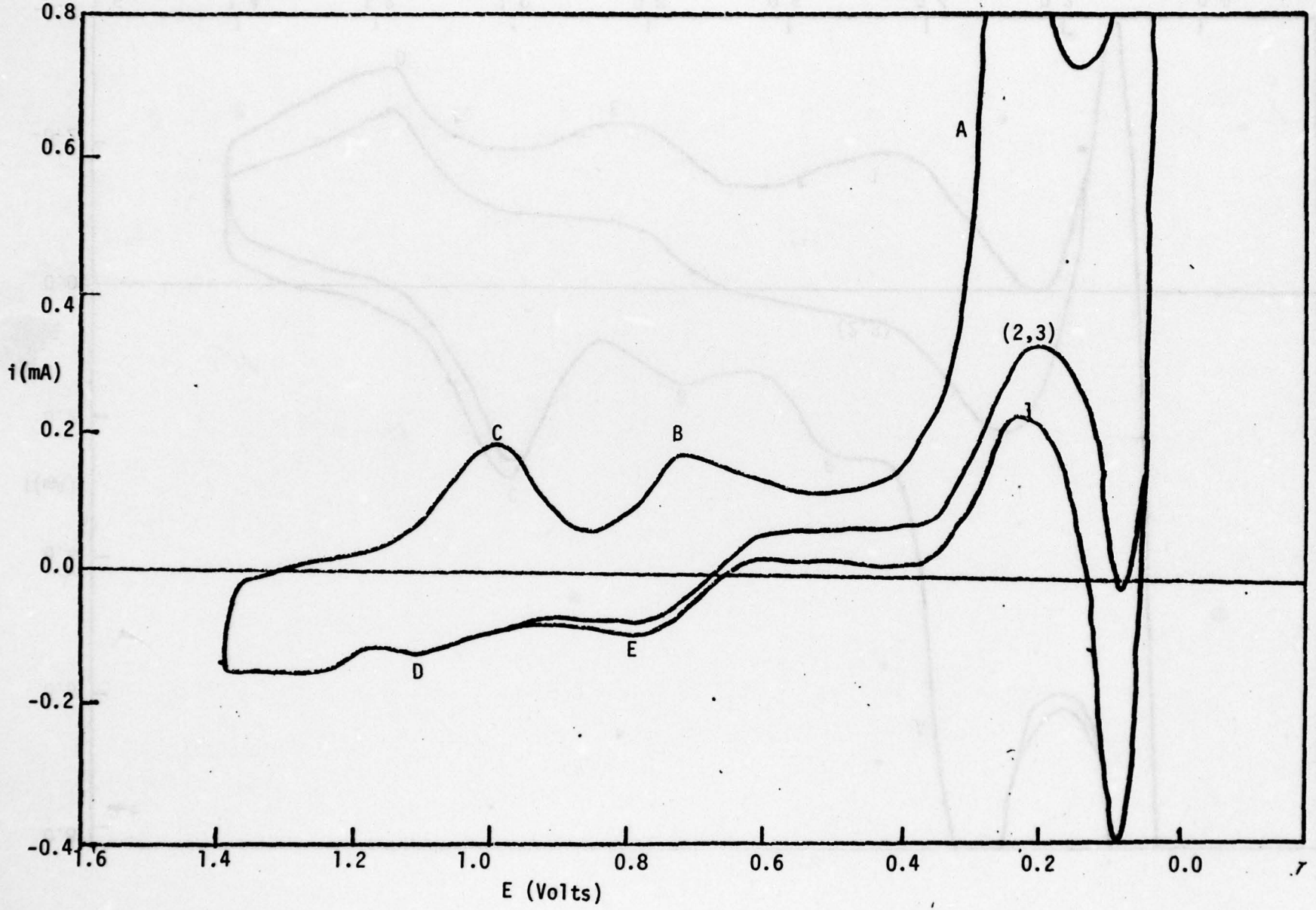

Figure 21. Current-Potential Curves in TFMSA After Potentiostating at 1.0 V

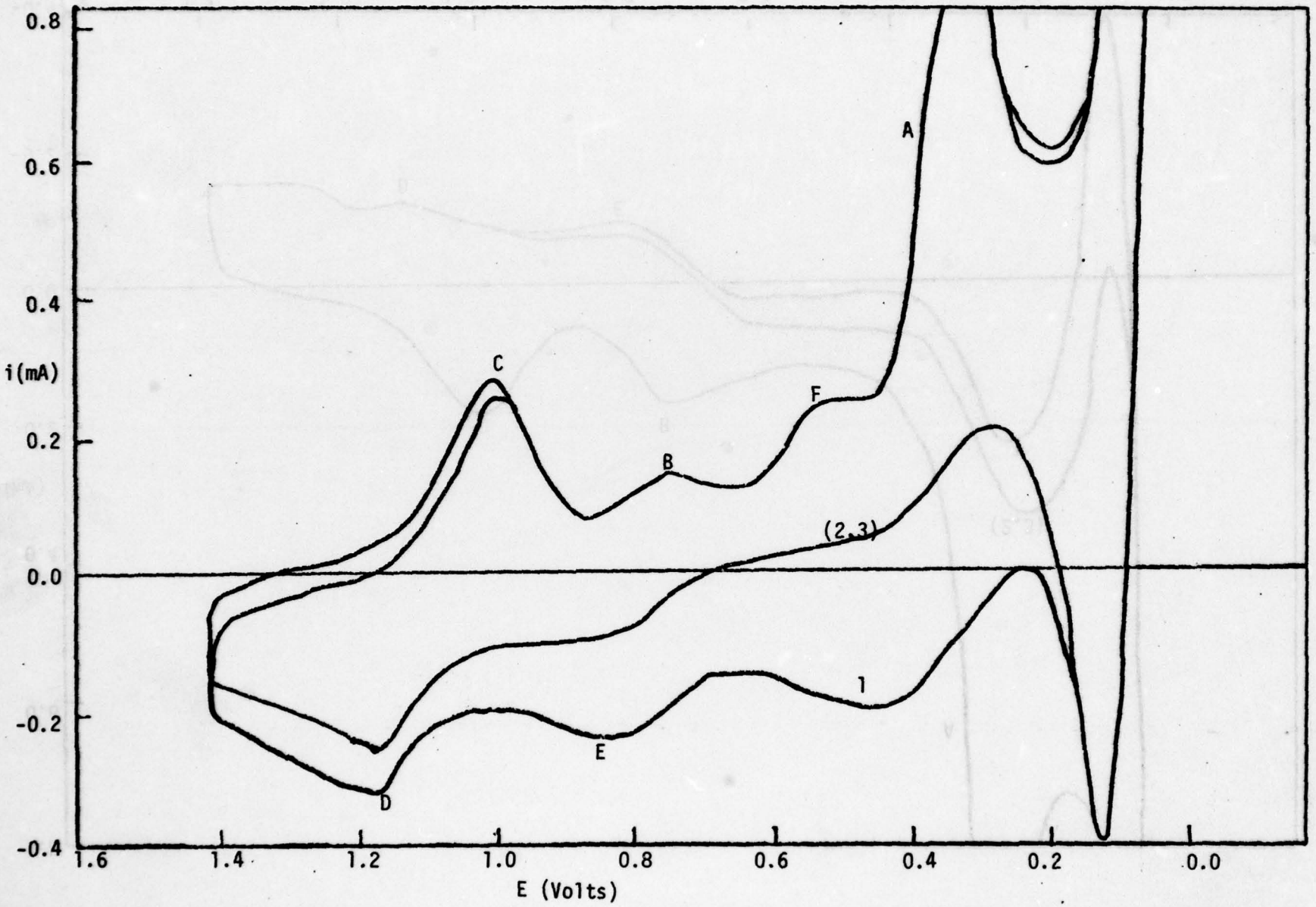

Figure 22. Current-Potential Curves in TFMSA After Potentiostating at 0.4 V.

potential range which gradually decreased to the residual current of fresh TFMSA as shown in Curves 2 and 3. This initial anodic current is believed to result from platinum oxidation which was previously shown to occur over a wide potential range. By jumping from the set potential to 0.0 V momentarily before the first anodic scan, more platinum is reduced on the electrode than by the normal scan, causing the initial anodic current observed in these multiple scan experiments.

Peak F was detected in the current i-E curve of Figure 22, but was not detected in Figure 21. Peak F was shown to be a mass transfer controlled process, but it's cause is unknown.

From these linear potential scan experiments, it is seen that platinum is easily oxidized in TFMSA over a wide potential range. Potential cycling the platinum electrode several times produced peak A, due to the reduction of platinum dissolved in the solution adjacent to the electrode.

The linear scan experiments indicate the complexity the TFMSA electrolyte system. Complete analysis of various processes would require considerably more effort and time than appears to be warranted.

CHAPTER V

CONCLUSIONS

Several serious problems with propane oxidation using $PtIEM_{TFMSA}$ electrodes were uncovered by these studies.

First, lower than anticipated propane electrooxidation current were found with the $PtIEM_{TFMSA}$ electrode. Comparing hydrogen to propane electrooxidation current, the hydrogen currents proved to be 145 times larger per mole of gas oxidized.

Second, conductance studies prove TFMSA to be a much weaker electrolyte than expected. The conductance in TFMSA was only one tenth that of 85% H_3PO_4.

Third, platinum, the electrocatalyst for propane oxidation dissolved significantly in TFMSA under the temperature and potential conditions which may occur in a propane fuel cell.

If a $PtIEM_{TFMSA}$ electrode is to be used for oxidation of propane in a fuel cell, considerably more work must be performed to demonstrate feasibility. First, a search for solutes or additives should be undertaken to determine whether the solvent resistance can be decreased. Thermally stable Lewis bases are one class of possible additives. Second, further studies on the solubility of platinum should be undertaken to establish the potentials at which a platinum anode could operate in TFMSA without appreciable platinum dissolution occurring.

CHAPTER VI

REFERENCES

1) W. T. Grubb and L. W. Niedrach, J. Electrochem. Soc., 110, 1086 (1963).

2) A. A. Adams and H. J. Barger, J. Electrochem. Soc., 121 , 987 (1974).

3) W. T. Grubb, Proc. 11th Ann. Battery Research and Development Conference, PSC Publications Committee, Red Bank, N.J., p. 5 (1957).

4) J. Giner, J. Electrochem. Soc., 111, 376 (1964).

5) D. F. Napp, D. C. Johnson, S. Bruckenstein, Anal. Chem., 39, 481 (1967).

6) F. G. Will and C. A. Knorr, Z. Electrochem. 64, 258 (1960).

7) Owen L. Davies, "Design and Analysis of Industrial Experiments", Hafner Publishing Company (1960).

8) W.G.F. Grot, G. E. Munn and P. N. Walmsley, "Perfluorinated Ion Exchange Membranes", 141st National Meeting of the Electrochemical Society, May 7-11, 1972.

9) R. G. Miekka, Natick, E. H. Lyons, Jr., Marblehead, R. M. Dempsey, U.S. Patent 3, 356, 538, Dec. 5 1967.

10) Lloyd E. Chapman, Intersoc. Energy Convers. Eng. Conf., Conf. Proc. 7th, p. 466 (1972).

11) I. M. Kolthoff and Philip J. Elving, "Treatise On Analytical Chemistry," Part II, Vol. 8, Interscience Publishers, 1963.

12) T. M. Riedhammer, S. Bruckenstein, Report to USAMERDC, Contract DAAK02-71-C-0306, June 1975.

DISTRIBUTION LIST

Commander (12)
Defense Documentation Center
Cameron Station, Bldg. 5
ATTN: TISIA
Alexandria, VA 22314

Chief (1)
Research, Development & Acquisition
Office, Deputy Chief of Staff
Department of the Army
Washington, DC 20310

Office of the Under Deputy Secretary (1)
of Defense (Research & Advanced Technology)
ATTN: ASST DIR, Electronics & Physical
Sciences
Washington, DC 20301

Director, Technical Information (1)
Advanced Research Projects Agency
1400 Wilson Blvd
Arlington, VA 22209

Commander (1)
US Army Materiel Development
and Readiness Command
ATTN: DRCDE-D
5001 Eisenhower Avenue
Alexandria, VA 22333

Commander (1)
US Army Tank-Automotive R&D Command
Technical Library/DRDTA-UL
Warren, MI 48090

Commander (1)
US Army Electronics R&D Command
ATTN: DRSEL-TL-P
Fort Monmouth, NJ 07703

Commander (1)
US Army Transportation Research &
Engineering Command
ATTN: Research Directorate
Fort Eustis, VA 23604

Chief (1)
US Army Security Agency
Arlington Hall Station
Arlington, VA 22212

Technical Documents Center (2)
US Army Mobility Equipment R&D Command
ATTN: DRDME-WC
Fort Belvoir, VA 22060

Chief (1)
Naval Ships Engineering Center
Department of the Navy
ATTN: Code 6157D, Mr. Albert Himy
Washington, DC 20362

Director, Power Branch (1)
Office of Naval Research
ATTN: 473
800 Quincy Street
Arlington, VA 22217

Department of the Navy (1)
Office of Naval Research
Ballston Tower #1
800 N. Quincy Street Code: 472 Room 624
Arlington, VA 22217

Commander (1)
Naval Ordnance Test Station
China Lake, CA 93555

Commander (1)
Naval Electronics Laboratory Center
ATTN: Research Library
San Diego, CA 92152

Director (1)
US Naval Research Laboratory
ATTN: Code 2027
Washington, DC 20390

Commander (1)
Aerospace Power Division
ATTN: AFAPL/PO (Mr. J.D. Reams)
Wright-Patterson Air Force Base
Dayton, OH 45443

Commander (1)
Department of the Air Force (AFSC)
Rome Air Development Center
ATTN: RBEG, (Mr. F.J. Mollura)
Griffiss AFB, NY 13441

Commander (1)
AFEWC (SURP)
San Antonio, TX 78241

DISTRIBUTION LIST

Power Information Center (1)
University City Science Center
3624 Science Center
Philadelphia, PA 19104

Director (1)
George Marshall Space Flight Center
ATTN: Mr. J.L. Miller (M-ASTR-E)
Huntsville, AL 38809

Director (1)
Lewis Research Center
National Aeronautics & Space Administration
ATTN: Mr. H.J. Schwartz (M.S. 309-1)
21000 Brook Park Road
Cleveland, OH 44135

Dr. Paul Nelson, Director (1)
Argonne National Laboratory
Bldg 205
9700 South Cass Avenue
Argonne, IL 60439

Mr. Norman Rosenberg (1)
US Department of Transportation
Transportation Systems Center
55 Broadway
Cambridge, MA 02142

US Department of Energy (1)
ATTN: Mr. Gary Voelker
20 Massachusetts Avenue, NW
Washington, DC 20545

Dr. Paul Milner (1)
Room 1D-259
Bell Telephone Laboratories
Murray Hill, NJ 07974

Electrochimica Corporation (1)
2485 Charleston Road
ATTN: Technical Library
Mountain View, CA 94040

Engelhard Industries Division (1)
Engelhard Minerals & Chemicals Corp
Government Services Department
70 Wood Avenue, South
Metro Park Plaza
ATTN: V.A. Forlenza
Iselin, NJ 08830

Mr. George Ciprios (1)
Exxon Research & Engineering
PO Box 8
Linden, NJ 07036

General Electric Company (1)
50 Fordham Road
ATTN: L.J. Nuttall
Bldg. 1A
Wilmington, MA 01887

P.L. Howard Associates, Inc (1)
Millington, MD 21561

Power Systems Division (1)
United Technologies Corporation
PO Box 109
Governor's Highway
South Windsor, CT 06074

Power Systems Division (1)
United Technologies Corporation
ATTN: Dr. H. Russel Kunz
PO Box 109, Governor's Highway
South Windsor, CT 06074

Occidental Research Corporation (1)
ATTN: Herbert P. Silverman
PO Box 310, Department 2-K
LaVerne, CA 91750

Union Carbide Corporation (1)
Parma Research Center
PO Box 6166
ATTN: Dr. R. Brodd
Parma, OH 44101

Energy Research Corporation (1)
ATTN: Dr. B.S. Baker
3 Great Pasture Road
Danbury, CT 06810

Dr. S.B. Brummer (1)
Director of Physical Research
EIC, Inc.
55 Chapel Street
Newton, MA 02158

Electric Power Research Institute (1)
ATTN: A.P. Fickett
PO Box 10412
Palo Alto, CA 94304

DISTRIBUTION LIST

Dr. Ralph Roberts (1)
Energy Resources & Environmental Systems
Engineering
The MITRE Corporation
Mail Stop W-389
Westgate Research Park
McLean, VA 22101

Universal Oil Products, Inc. (1)
Ten UOP Plaza
ATTN: Stephen N. Massie
Government Contract Administrator
Des Plains, IL 60016

Technology Center (1)
ESB Incorporated
19 W College Avenue
ATTN: Dr. D.T. Ferrell, Jr.
Yardley, PA 19067

Dr. Paul Stonehart (1)
Stonehart Associates, Inc.
34 Five Fields Road
Madison, CT 06443

Dr. Jose Giner (1)
Giner, Inc.
14 Spring Street
Waltham, MA 02154

Massachusetts Institute of Technology (1)
ATTN: Professor H.P. Meissner
Cambridge, MA 02138

Dr. Douglas N. Bennion (1)
Energy & Kinetics Department
School of Engineering & Applied Science
5532 Boelter Hall
University of California
Los Angeles, CA 90024

University of Florida (1)
Department of Chemical Engineering
PO Box 3027
ATTN: Professor R.D Walker
Gainsville, FL 32601

L.G. Marianowski (1)
Manager, Energy Conversion & Storage
Research
Institute of Gas Technology
3424 S. State Street
Chicago, IL 60616

Dr. R.T. Foley (1)
Chemistry Department
The American University
Washington, DC 20016

State University of New York at Buffalo (1)
ATTN: Professor Stanley Bruckenstein
Chemistry Department
Acheson Hall, SUNY/AB
Buffalo, NY 14214

Hugh J. Barger, Jr. (1)
Box 2232
Davidson, NC 28036


79